Aerosol and Air Quality Research, 19: 2130–2150, 2019

ISSN: 1680-8584 print / 2071-1409 online
doi: 10.4209/aaqr.2019.04.0215

Removal of Typical Industrial Gaseous Pollutants: From Carbon, Zeolite, and Metal-organic Frameworks to Molecularly Imprinted Adsorbents

Yan Huang[1], Wenhui Su[1], Rui Wang[1*], Tiansheng Zhao[2]

[1] *School of Environmental Science and Engineering, Shandong University, Jinan 250199, China*
[2] *State Key Laboratory of High-Efficiency Utilization of Coal and Green Chemical Engineering, Ningxia University, Yinchuan 750021, China*

ABSTRACT

In recent years, various adsorbents have been developed to alleviate atmospheric pollution and remove harmful gases, such as carbon dioxide, sulfur dioxide, nitrogen oxides, hydrogen sulfide and volatile organic compounds. Polymer-based adsorbents are a novel type of material now being used for gas separation and purification; in particular, molecular imprinted polymers (MIPs) can achieve selective adsorption of target gas molecules. However, existing review papers have not yet discussed the application of MIPs in gas purification. In this paper, therefore, we exhaustively summarize recently developed adsorbents, including the materials based on carbon, zeolite, and metal-organic frameworks as well as MIPs, to analyze the status of these materials and identify promising adsorbents for gas purification.

Keywords: Adsorption; Industrial gas; Molecule imprinting technique; Porous materials; Selectivity.

INTRODUCTION

Currently, 85% of demanded energy is supplied by thermal power plants that use fossil fuels (Akinyele *et al.*, 2014). However, these processes generate a considerable amount of hazardous gases, such as carbon dioxide (CO_2), sulfur dioxide (SO_2), hydrogen sulfide (H_2S), nitrogen oxides (NO_x), and volatile organic compounds (VOCs). The methods of capturing CO_2 can be categorized to pre-combustion and post-combustion capture (Jiang *et al.*, 2019; Pai *et al.*, 2019). Air pollution caused by SO_2 has received considerable research attention recently because of its contributions in the forms of acid rain and secondary pollutants (Li *et al.*, 2018). H_2S is so toxic and corrosive that the U.S. Environmental Protection Agency (EPA) reported corrosion of concrete wastewater pipes (due to H_2S) at a rate of 3.6 m^2 $year^{-1}$, and of sewer pipes at a rate of 2.5–10 m^2 a^{-1} (Habeeb *et al.*, 2017). NO_x has severe effects on the global ecosystem, particularly on human health. In addition, VOCs are the precursors of particles and ozone.

Therefore, separation and removal approaches, mainly adsorption and catalysis, have been developed to remove harmful gases. Among them, the adsorption method using solid adsorbents as separation media has been widely used in processes such as airflow drying, hydrogen purification, and nitrogen and oxygen production (Sevilla and Fuertes, 2012; Huang and Wang, 2018; Pai *et al.*, 2019). Traditional adsorbents have poor active sites, selectivity, and regeneration properties. Therefore, developing novel adsorbents with excellent properties is necessary for highly effective removal of these gases.

Molecular imprinting technique (MIT) is an interdisciplinary method that integrates polymer chemistry, materials science, chemical engineering and biochemistry. Molecularly imprinted polymers (MIPs) can be used to identify specific target molecules by mimicking the interaction between enzyme and substrates. According to the binding forms between templates and functional monomers, MIT can be categorized into covalent, noncovalent, and semicovalent methods. Covalent methods are also referred to as pre-organized methods, in which templates and functional monomers form precomplexes through covalent bonds (Shin *et al.*, 2018). Noncovalent methods are also called self-assembly methods, in which templates and functional monomers form precomplexes through noncovalent bondsthrough hydrogen bonding, electrostatic attraction, charge transfer, ion-pair interactions, metal coordination, hydrophobic interactions, and van der Waals forces (Shin *et al.*, 2018).

MIPs are a type of polymer material with a built-in recognition property that can be purposefully designed by changing templates, functional monomers, cross-linkers and initiators (Boysen, 2018). In other words, the polymerization

* Corresponding author.
Tel.: +86-531-88366367
E-mail address: wangrui@sdu.edu.cn

processes of MIPs can be divided into three stages, as indicated in Fig. 1. First, prepolymers form between templates and functional monomers. They are subsequently chemically fixed by cross-linkers to create three-dimensional (3D) polymer networks. Finally, template molecules are removed from the polymers, thus producing specific cavities. MIPs have the advantages of simple preparation, high selectivity and easy regeneration because of a lot of active sites with spatial shapes and sizes similar to those of templates (Ying and Nan, 2010). They have been studied in a wide range of fields, such as adsorption, solid-phase extraction, catalysis, sensors, and electron probes (Cheong *et al.*, 2013; Xu *et al.*, 2019).

This study reviews advances in the development of absorbents for gas removal. Emphasis is placed on functional adsorbents, such as MIPs and carbon-based, zeolite-based, and metal-organic framework (MOF) materials, as well as their selectivity and separation properties.

ADSORPTION AND CAPTURE OF COMMON GASES

Carbon Dioxide

Major sources of CO_2 are thermoelectric power plants and industrial plants, which account for approximately 45% of CO_2 emissions (Lee and Park, 2015; Beidari *et al.*, 2017). Many successful technologies have been developed and applied for CO_2 capture, such as solvent absorption, chemical or physical adsorption, membrane separation, and cryogenic separation (Santiago *et al.*, 2018). In addition, novel adsorbents have also been developed to reduce CO_2 emissions, as indicated in Table 1. These adsorbents are capable of capturing and storing CO_2 to directly reduce the CO_2 emissions from operational coal power plants (Tobiesen *et al.*, 2018; Wawrzyńczak *et al.*, 2019). Rezakazemi *et al.* (2019) conducted CO_2 adsorption experiments using nanofluids in a gas-liquid hollow fiber membrane contactor and analyzed the results with a two-dimensional (2D) mathematical model. Simulation results revealed that the adsorption rate of 0.05 wt% SiO_2 nanoparticles increased to 16%. However, using a 0.05 wt% carbon nanotubes (CNTs) increased the adsorption rate by up to 34%. This result suggested that CNTs have markedly superior adsorption capacity and hydrophobicity compared with SiO_2 nanoparticles. Louis *et al.* (2018) reported that membrane capacitive deionization (MCDI) could be used to capture CO_2 as bicarbonate and carbonate ions produced by the reaction of CO_2 and water at room temperature and atmospheric pressure. In this process without using chemicals, the absorption-desorption behavior of CO_2 can be driven by the adsorption and desorption of bicarbonate ions from water.

Activated Carbons

Marszewska and Jaroniec (2017) prepared highly-porous carbon spheres by combining silica template and CO_2 activation. The experimental results showed that mesoporosity could improve mass transfer, leading to high and fast CO_2 adsorption, and the CO_2 adsorption capacity reached 4.0 mmol g^{-1} at 23°C and 1 bar. Ogungbenro *et al.* (2018) studied activated carbon synthesized from jujube seeds prevalent in the United Arab Emirates (UAE) for CO_2 adsorption. The results suggested that the adsorbent with rich pores had high CO_2 adsorption capacity of 141.14 mg g^{-1} at room temperature. Tehrani *et al.* (2019) prepared nitrogen-sulfur-doped nanoporous carbon with a

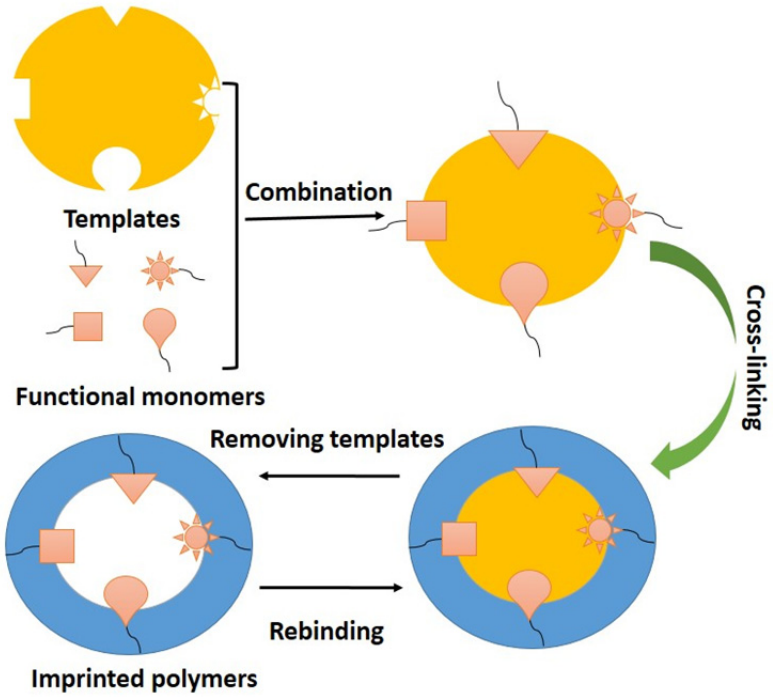

Fig. 1. Schematic of the preparation of imprinted polymers (Huang and Wang, 2018).

Table 1. Functional adsorbents for CO_2 removal.

Adsorbents	mg CO_2 g^{-1} adsorbent	T (°C)	composition	Ref.
AC-$ZnAC_2$	63.61	room temperature	CO_2 in H_2	Sevilla and Fuertes (2012)
N-S-rich nanoporous carbon	7.15	25	CO_2/CH_4	Sidek *et al.* (2019)
NC-Cu-BTC	8.24	0	CO_2 in N_2	Zhao *et al.* (2015)
	4.51	25		
zeolite/activated carbon honeycomb	1.2	20	CO_2 in N_2	Belmabkhout *et al.* (2010)
hierarchical carbon nanosheet-based networks (GPC)	4.62	0	CO_2 in N_2	Chen *et al.* (2010)
Ni (II)-Mofs	118.2	30	CO_2/N_2	An *et al.* (2009)
MIL-91(Al)	2.4	25	CO_2/N_2	Zhao *et al.* (2014)
HKUST-1	102.6	25	CO_2/N_2	Nabavi *et al.* (2017)
MOF-591	36	25	CO_2/N_2	He *et al.* (2016)
MOF-592	42	25	CO_2/N_2	He *et al.* (2016)
unconventional MOFs	0.86	25	CO_2/N_2	Gupta *et al.* (2016)
PCN-250(Fe_3)	1.82	25	CO_2/N_2	Chen *et al.* (2018b)
Inorganic-organic composite sorbent	4.54	25	CO_2 in H_2O	Nowicki *et al.* (2014)
hexagonal mesoporous silica	184	75	CO_2 in N_2	Xu *et al.* (2014)
PEI/monolith	210	75	CO_2 in N_2	Kazmierczak-Razna *et al.* (2015)
TEPA/monolith	260			
TEPA/MSU-1	3	75	CO_2 in N_2	Lau *et al.* (2015)
MIP Adsorbent	0.48	60	CO_2 in H_2O	Balsamo *et al.* (2016)
	0.49		CO_2 in O_2	
	0.57		CO_2 in SO_2	
	0.50		CO_2 in NO_x	
poly[acrylamide-co-(ethylene glycol dimethacrylate)] polymer particles	1.1	0	CO_2 in N_2	Lee *et al.* (2017)
IPEIA-R	8.56	25	CO_2 in H_2O	Sun *et al.* (2018)

large surface area of 2186 m^2 g^{-1} and pore volume of 1.3 cm^3 g^{-1}. CO_2 adsorption capacity reached 7.15 mmol g^{-1} at 1 bar and 25°C and reached 29.29 mmol g^{-1} at 35 bar and 25°C, indicating that pressure significantly influenced CO_2 absorption. Sidek *et al.* (2019) evaluated the CO_2 adsorption performance of activated carbon (AC) impregnated by zinc acetate in terms of breakthrough time and adsorption capacity. The maximum CO_2 adsorption capacity of the AC was 63.61 mg g^{-1}, and the longest breakthrough time was 25.7 min under the optimum feed gas flow rate of 0.25 L min^{-1}. Liu *et al.* (2019) designed novel composite adsorbents by combining a copper and benzene-1,3,5-tricarboxylate(-BTC) framework with a series of porous carbons, including ordered mesoporous non-activated carbon (OMC), ordered mesoporous AC, and nitrogen-containing microporous carbon (NC), and used these adsorbents to capture CO_2. Zhao *et al.* (2019) designed a new hybrid zeolite/AC honeycomb to achieve electrical swing adsorption for CO_2. When the power-on time was extended from 30 to 180 s, electrical swing adsorption achieved 15%–34% purity of CO_2 products and 29%–78% recovery rate. In a vacuum and electrical swing adsorption process, however, the CO_2 purity and recovery rate reached 33% and 72%, respectively, under the conditions of 10 kPa and electrochemical time of < 30 s. Zhang *et al.* (2018) prepared nitrogen-doped activated carbon (AC-N) using melamine as the nitrogen source and studied its catalytic performance for CO_2. The results revealed that AC-N had 60% and 75% conversion rates for methane (CH_4) and CO_2, respectively. Li *et al.* (2019) prepared AC from petroleum coke through the potassium hydroxide (KOH) chemical activation method. The results indicated that AC had a high adsorption capacity of CO_2 by volume. Different from the above adsorbents, Xie *et al.* (2017) studied the amine-modified carbon aerogel for CO_2 capture, and found that the maximum adsorption capacity was 2.06 mmol g^{-1} when the amine loading of carbon aerogel was 55 wt.%. Shao *et al.* (2018a) fabricated the porous carbon with the organic-inorganic hybrid framework thorough the direct carbonization and KOH-activation carbonization of triazine-based hyper-cross-linked polymers. Under the optimum preparation conditions, the surface area could attain 2058 m^2 g^{-1}. At 298 K and 10 bar, the adsorption capacity of the adsorbent for CO_2 was 590 mg g^{-1}. The CO_2/N_2 selectivity experiment suggested the best Henry's law $S_{CO2/N2}$ was 16.1. The result showed that the porous carbon with excellent surface area and microporosity structure had good adsorption and selectivity properties for CO_2.

Metal-organic Frameworks

MOFs have been studied for laboratory-scale applications such as gas separation, purification, storage, and heterogeneous catalysis. Zhao *et al.* (2015) discovered that some MOFs have favorable CO_2 capacity and high CO_2 selectivity with regard to dinitride (N_2). Pai *et al.* (2019) prepared five MOFs modified by diamine and evaluated post-combustion CO_2 capture from dry flue gas through a vacuum swing adsorption process. Among them, the mmen-Mn_2(dobpdc) and mmen-Mg_2(dobpdc) resulted in CO_2 purity and recovery of 95% and 90%, respectively. In the presence of N_2, these MOFs exhibited higher selectivity for CO_2. Gholidoust *et al.* (2019) discovered that compared with other solid physical adsorbents, some MOFs had higher CO_2 capture capacities under high pressure but poorer capacities at low CO_2 partial pressures. Elsabawy and Fallatah (2019) prepared an amorphous nickel-(II)-MOF with an ultrahigh BET surface area, and the maximum adsorption capacity was 118.2 mg CO_2 g^{-1} under the conditions of 30°C and 27 bar. Kong *et al.* (2018) synthesized a stable layered bisphosphonate, MIL-91(Al), for adsorbing CO_2 under various environmental conditions. The MIL-91(Al) exhibited a maximum adsorption capacity of 2.4 mmol g^{-1}, and higher selectivity for CO_2 than for N_2 and CH_4. Shalini *et al.* (2018) investigated the potential of MOFs to separate CO_2 from industrial-rich greenhouse gas mixtures. Silva *et al.* (2018) synthesized a new type of microporous zirconate material using formaldehyde as the solvent. When evaluated on the basis of ideal adsorption solution, the results revealed that the material had higher selective adsorption capacity for CO_2 than for N_2 and CH_4. Zhou *et al.* (2018b) modified the metal-organic skeleton (HKUST-1) by doping lithium to improve its CO_2 adsorption performance; the modified HKUST-1 with a moderate concentration of lithium nitrate solution as the dopant demonstrated the best adsorption capacity for CO_2. Nguyen *et al.* (2018) employed the solvothermal method to synthesize three new lanthanide MOFs, namely MOF-590, MOF-591, and MOF-592. Among them, MOF-590 exhibited best conversion efficiency (96%), selectivity (95%) and yield (91%). MOF-591 and MOF-592 had moderate CO_2 adsorption capacities of 36 and 42 cm^3 g^{-1}, respectively, at 800 Torr and 298 K.

Composite Materials

Amine-based chemical adsorption has been commercially used for CO_2 separation in the natural gas industry (Rayer *et al.*, 2018). Chen *et al.* (2009, 2010) synthesized a series of hexagonal mesoporous silica (HMS) materials with different textural porosities by using dodecylamine as a structure-directing agent and loaded polyethylenimine (PEI) on the surface of HMS to prepare PEI/HMS adsorbents for CO_2 capture. They found that PEI/HMS adsorbents exhibited a CO_2 capture capacity superior to that of other silica-supported amine sorbents and had adequate regeneration performance. Wang *et al.* (2011) proposed tetraethylenepentamine (TEPA)/MSU-1, which was prepared by incorporating TEPA with self-prepared mesoporous silica MSU-1 using cheap sodium silicate as the silica source; they discovered that the TEPA/MSU-1 has a high adsorption capacity for CO_2. Lai *et al.* (2018) prepared an inorganic-organic composite solid sorbent by using aminoethylethanolamine to impregnate nanoporous silicic acid and thereby capture CO_2 from flue gas. In another study, PEI was immobilized in a silica substrate to capture CO_2 through a pressure swing adsorption process (An *et al.*, 2009).

Recently, Zhao *et al.* (2014) synthesized molecularly imprinted CO_2 adsorbents (CO_2-MIPs) by using ethanedioic acid, acrylamide, and ethylene glycol dimethacrylate as the template, functional monomer, and cross-linker, respectively.

They investigated the CO_2-MIPs' ability to separate CO_2 from coal-fired flue gas after desulfurization; under the optimum adsorption temperature of 60°C, the maximum adsorption capacity of CO_2 was 0.57 mmol g^{-1}. The researchers also prepared a series of CO_2-MIPs by employing the molecular self-assembly method. They discovered that MIP1b with a high amine content demonstrated favorable CO_2 capacity compared with MIP3 and remained stable after 50 adsorption-desorption cycles. In an atmosphere of 15% CO_2 and 85% N_2, the CO_2 separation coefficients of all adsorbents were over 100 (Zhao *et al.*, 2012). Nabavi *et al.* (2017) also synthesized CO_2-MIPs in oil-in-oil emulsion through suspension polymerization. The CO_2-MIPs had selectivity of 49% for CO_2/N_2 at 0.15 bar CO_2 partial pressure, and of 97% at ultralow CO_2 partial pressure. Liu *et al.* (2018b) synthesized molecularly imprinted solid amine adsorbents through a simple cross-linking reaction by using PEI as the framework, glycidyl ether as the cross-linker, and a CO_2 molecule as the template. The synthesis process of the molecularly imprinted solid amine adsorbent is displayed in Fig. 2. The amine content of MIP-PEI reached 11.41 mmol g^{-1}, but the diffusion resistance of CO_2 was low during the CO_2 adsorption process. The adsorption capacity of MIP-PEI for CO_2 (6.58 mmol g^{-1}) was higher than that of nonimprinted NIP-PEI (5.87 mmol g^{-1}). Water significantly improved the adsorption capacity of CO_2 by promoting the chemical adsorption of CO_2 on solid amine adsorbents. He *et al.* (2016) prepared a CO_2-imprinted solid amine adsorbent, and the adsorption results revealed that the imprinting of sodium borohydride ($NaBH_4$) on CO_2 and the reduction of imino groups led the adsorbent to have a high adsorption capacity for CO_2. The solid amine adsorbent based on PEI exhibited a remarkable CO_2 adsorption capacity of 8.56 mmol g^{-1} in the presence of water at 25°C, which was attributed to its high amine content and strong swelling performance. The regeneration experiment revealed that the CO_2 adsorption capacity remained unchanged after 15 adsorption-desorption cycles, suggesting that the prepared adsorbents had adequate regeneration performance.

In the future, CO_2 will be one of the most important energy sources because it has the potential to be converted into various value-added chemicals, such as methanol, formic acid, carbonates, and carboxylic acid (Yang and Wang, 2015). However, the concentration of CO_2 in the industrial gases is too low and cannot meet the reaction requirement of catalytic conversion. Therefore, developing cheap and functional adsorbents with highly effective adsorption and catalytic properties is the key research direction to develop new and enabling processes. As a whole, new functional adsorbents, cheap and readily available, environment-friendly, selective and reusable, are desirable.

Hydrogen Sulphide

H_2S, which is an odorous, poisonous, and corrosive gas, is found in many industrial fields, such as oil production, coal gasification, natural gas, digester gas, and metal smelting (Liu and Wang, 2017a). The use of H_2S not only hinders industrial production and leads to high running costs but also has considerable effects on human health, such as headaches, dyspnea, dizziness, and even asphyxiation, loss of consciousness, and fatality (Gupta *et al.*, 2016). The Occupational Safety and Health Administration (OSHA) categorized H_2S concentrations into three levels of toxicity: 10 ppm or less denotes low toxicity, between 10 ppm and 30 ppm is considered medium toxicity, higher than 30 ppm is high toxicity for humans (OSHA, 2015). Therefore, the removal of H_2S would considerably influence industrial production, environmental quality and the occurrence of human health problems. In addition, raw industrial gases commonly contain H_2S, CO_2, CH_4 and other light alkanes. Among the methods used to remove H_2S, adsorption is regarded as one of the most suitable approaches because of the advantages of low running costs, low corrosion and

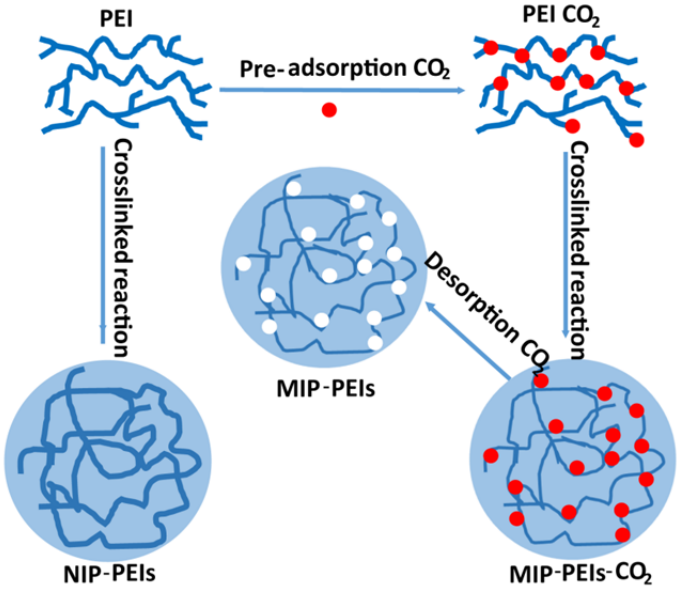

Fig. 2. The synthesis process of molecularly imprinted solid amine adsorbent (Liu *et al.*, 2018).

flexibility. In recent years, novel functional adsorbents have been widely studied for their ability to achieve H_2S selective separation and removal; as indicated in Table 2, these adsorbents include MOF-based, carbon-based, zeolite-based, metal oxide-based, and composite materials.

Carbon-based Functional Materials

AC with abundant pore channels is a well-known adsorption material that can be easily prepared through the carbonization of biomass such as wood, coconut shells and straw. Nowicki *et al.* (2014) prepared carbonaceous materials by using coffee industry waste and found that an appropriate amount of steam promoted H_2S adsorption. Xu *et al.* (2014) also proved that the introduction of steam increased the adsorption capacity of AC for H_2S; the adsorption capacities of AC from sewage sludge and pig manure increased from 43.9 and 59.6 to 47.5 and 65.5 mg g^{-1}, respectively, under a 25wt% humidity. For safer and easier AC preparation, Kazmierczak-Razna *et al.* (2015) utilized sawdust pellets to synthesize AC through microwave radiation. However, the adsorption capacity of the prepared AC for H_2S was 6.2 mg g^{-1}, which may be caused by its low surface area of 426 m^2 g^{-1}. Lau *et al.* (2015) prepared AC derived from palm shell by loading cerium oxide (CeO_2) and sodium hydroxide (NaOH) to remove H_2S from biogas, and the adsorbent exhibited adequate removal capability for H_2S in the presence of CO_2 and CH_4. To enhance the interaction between the carbon surface and H_2S, Yu *et al.* (2015) introduced N heteroatoms into the carbon matrix, thereby obtaining nitrogen-doped porous carbons (NPCs) by using D-glucose and melamine as the carbon source and nitrogen source, respectively. The binding energy result demonstrated that the interaction between pyridinic N and H_2S (–14.6 kJ mol^{-1}) was greater than that at the raw carbon surface (–1.8 kJ mol^{-1}). Fauteux-Lefebvre *et al.* (2015) prepared iron-functionalized carbon nanofilaments (Fe-CNFs) to study their removal ability for H_2S at low (100°C) and high (300°C) temperatures. The CNFs acted as not only a sulfur adsorbent but also the carrier for evenly dispersing the iron, which had two roles in the Fe-CNFs: at 100°C, it enhanced the H_2S retention capacity of the CNFs, and at 300°C, it reacted with H_2S to form iron sulfide. Balsamo *et al.* (2016) studied the H_2S removal property of AC loaded with Zn and Cu and demonstrated that functional AC had superior adsorption ability to that of raw AC. Temperature-programmed desorption of the saturated adsorbents revealed that a combination of H_2S adsorption and oxidation led to the formation of metal sulfates, thus exhibiting surface reaction complexity. Lee *et al.* (2017) used goethite (α-FeOOH) to modify AC for H_2S removal from a gas stream. The composite adsorbent had superior removal ability, which is because the introduction of AC as support prevented the agglomeration of α-FeOOH and further increased the utilization rate of active sites. Goncalves *et al.* (2018) evaluated the H_2S adsorption capacities of ACs with different pore sizes from monocomponent H_2S and mixture gases of H_2S, CO_2 and CH_4 and discovered that CO_2 promoted H_2S adsorption in AC with 8.9 Å pores. To achieve the effective regeneration of adsorbents, Farooq *et al.* (2018) applied a new regeneration method, electric potential swing desorption, for the regeneration of saturated AC; this method resulted in H_2S desorption that was three times faster than that resulting from the nonpotential desorption method. In addition, structured carbons, including CNTs and graphene-based materials, are mainly applied in sensor research to detect H_2S (Asad and Sheikhi, 2014; Choi *et al.*, 2014; Duong-Viet *et al.*, 2016; Song *et al.*, 2016; Chu *et al.*, 2018; Liao *et al.*, 2018).

Zeolite-based Functional Materials

As a type of porous crystalline material, zeolites have the advantages of high surface area and regular pore size and shape, which have led to their wide application in the fields of adsorption and catalysis. For desulfurization, zeolite-based materials are mainly used as adsorbents because of their high sulfur capacity, strong regeneration performance, and stable structure. Tomadakis *et al.* (2011) studied the H_2S separation properties of 4A, 5A, and 13X molecular sieves from CO_2 through pressure swing adsorption. They discovered that the fresh 13X sieves exhibited the highest separation factor (11.9) for H_2S/CO_2 compared with the 5A (5.4) and 4A (2) zeolites. Maghsoudi *et al.* (2013) first investigated the adsorption ability of pure silica chabazite (Si-CHA) for H_2S, CO_2 and CH_4, reporting that the adsorption capacity in order was $H_2S > CO_2 > CH_4$ and that the H_2S capacity was 4 mmol g^{-1} at 25°C and 2 bar. Shah *et al.* (2015) investigated the separation of seven all-silica zeolite frameworks (CHA, DDR, FER, IFR, MFI, MOR and MWW) for H_2S/CH_4 through Gibbs ensemble Monte Carlo simulations. When the H_2S concentration was low, MOR exhibited the highest selectivity and the most favorable enthalpy of adsorption for H_2S; this was attributed to the favorable interactions between H_2S and adsorbents in its smaller pores. However, MFI demonstrated the highest degree of selectivity for H_2S at a high H_2S concentration (Shah *et al.*, 2015). To improve the H_2S removal capacity of zeolite, Liu *et al.* (2015a) prepared a material with the dual functions of adsorption and photocatalysis by combining zeolite with titanium dioxide (TiO_2). The adsorbent had selective removal ability for H_2S and could be effectively regenerated through calcination. Hao *et al.* (2016) also investigated the H_2S removal ability of TiO_2-zeolite, and the material exhibited an excellent H_2S removal rate (97%) and low SO_2 selectivity (9.2%). Sigot *et al.* (2016b) studied the regeneration property of 13X zeolite through thermal desorption and discovered that zeolite had poor desorption behavior at a lower temperature (350°C) in an inert atmosphere. From an industrial perspective, Liu and Wang (2017b) used cheap attapulgite to synthesize a 4A molecular sieve from zeolite for H_2S removal. The experimental result indicated that the zeolite had a higher sulfur saturation capacity of 12.4 mg g^{-1} at 50°C compared with pure sieves, and the saturated 4A zeolite could be effectively regenerated through N_2 purging at 350°C; moreover, the highest removal rate for H_2S could be maintained at 100 % in every cycle experiment. Similarly, Abdullah *et al.* (2018) utilized local kaolin as the alumina and silica source

Table 2. Functional adsorbents for H_2S removal.

Adsorbents	mg H_2S g^{-1} adsorbent	T (°C)	composition	Ref.
AC from coffee waste	281.5	room temperature	0.1% H_2S in air	Asad and Sheikhi (2014)
AC from sewage sludge	47.5	room temperature	1% H_2S in air	Liao *et al.* (2018)
AC from pig manure	65.4			
CeO_2/NaOH/AC from palm shell	187.1	30	H_2S in CO_2/CH_4	Song *et al.* (2016)
NPCs	42.6	25	H_2S	Chu *et al.* (2018)
Darco AC	6.8	30	H_2S in N_2	Maghsoudi *et al.* (2013)
$Cu_0Zn_{1.0}$/AC	33.1		H_2S in N_2	
$Cu_{0.05}Zn_{0.95}$/AC	43.6		H_2S in N_2	
$Cu_{0.1}Zn_{0.9}$/AC	44.6		H_2S in N_2	
$Cu_{0.25}Zn_{0.75}$/AC	46.3		H_2S in N_2	
$Cu_{0.5}Zn_{0.5}$/AC	49.7		H_2S in 40% CH_4	
$Cu_{0.5}Zn_{0.5}$/AC	48.4		H_2S in 40% CO_2	
$Cu_{0.5}Zn_{0.5}$/AC	51.1			
α-FeOOH/AC	171	room temperature	H_2S in N_2	Shah *et al.* (2015)
Cu/AC from rice husk	410.8	20	H_2S in N_2	Huang *et al.* (2015)
AC from tobacco stem	231.3	60	1% H_2S in N_2	Sigot *et al.* (2016a)
zeolite	1.7	25	0.1% H_2S	Cara *et al.* (2018)
TiO_2	2.0			
3% TiO_2/zeolite	3.4			
5% TiO_2/zeolite	4.4			
8% TiO_2/zeolite	5.1			
50%1Zn2Fe2Mn/MCM-48	140.3	550	0.33% H_2S, 10.5% H_2, 18% CO in N_2	Kim *et al.* (2014)
0.10Co/NaX zeolite	4.2	600	H_2S in N_2	Wu *et al.* (2018)
0.15Co/NaX zeolite	4.4			
13X zeolite	142	room temperature	H_2S in N_2	Cimino *et al.* (2018)
Coal-based IAC	785			
5Ce5Mn/ZSM-5	260.8	750	H_2S in N_2	Hamon *et al.* (2011)
4A zeolite from attapulgite	7.5	25	H_2S in N_2	Nickerl *et al.* (2014)
	8.4	50		
	6.5	75		
γ-Fe_2O_3/MCM-41	40.4	300	H_2S in He	Huang *et al.* (2012)
ZnO/Na-A zeolite	16.7	28	H_2S in N_2	Li *et al.* (2014)
Cu/13X zeolite	40	120	H_2S in N_2	Song *et al.* (2011)
Ag/NaX zeolite	52.1	25	H_2S, COS, CO_2 in N_2	Lange *et al.* (2015)
MCM-41@ZIF-8	5228	30	H_2S in N_2	Al-Jadir and Siperstein (2018)
SBA-15@ZIF-8	5536			
UVM-7@ZIF-8	6504			
Cu-Zn/SBA-15	85	150	H_2S in He	Bhatt *et al.* (2017)
ZnAl-MMO	318.8	600	H_2S, CO, H_2, O_2 in N_2	Liu *et al.* (2017)

Table 2. (*continued*).

Adsorbents	mg H_2S g^{-1} adsorbent	T (°C)	composition	Ref.
γ-Al_2O_3	3.1	30	H_2S in N_2	Liu *et al.* (2018)
$Cu_0Zn_{1.0}/\gamma$-Al_2O_3	23.2			
$Cu_{0.05}Zn_{0.95}/\gamma$-$Al_2O_3$	23.5			
$Cu_{0.1}Zn_{0.9}/\gamma$-Al_2O_3	24.9			
$Cu_{0.25}Zn_{0.75}/\gamma$-$Al_2O_3$	25.2			
$Cu_{0.5}Zn_{0.5}/\gamma$-Al_2O_3	27.9			
MOF-5/GO	130.1	20	H_2S in N_2	Wang *et al.* (2014)
MOF-199	43.3	30	H_2S in N_2	Cao *et al.* (2014)
MIL-101	153.3	25	H_2S in He	Guo *et al.* (2018)
MIL-101@30% carbon	119.3			
Y-FTZB-fcu-MOF	30.7	25	H_2S, CO_2 in N_2	Sun *et al.* (2014)
Y-fum-fcu-MOF	37.5			
Y-1,4-NDC-fcu-MOF	51.1			

instead of pure chemicals to synthesize low-cost Na-A zeolite and then introduced zinc oxide (ZnO) into its pore channels to remove H_2S from the biogas. On the basis of previous on NaX zeolite, Chen *et al.* (2018a) used Zn, Co, and Ag to modify NaX zeolite though the ion-exchange method; the NaX modified by Ag had the highest adsorption capacity for H_2S (1.53 mmol g^{-1}). Tran *et al.* (2016) also investigated Co-doped NaX zeolite. To study the effects of the pore structures and wall thickness of zeolites on H_2S removal, Cara *et al.* (2018) used maghemite (γ-Fe_2O_3). modified hexagonal MCM-41 and cubic MCM-48. They discovered that the adsorbent based on hexagonal MCM-41 had more stable adsorption and superior regeneration performance compared with that based on cubic MCM-48.

Metal Oxide-based Functional Materials

In solid adsorbents for H_2S removal, the reaction temperatures of carbon-based materials are relatively low; nevertheless, the desulfurization process is discontinuous. Although their reaction temperatures are relatively high, metal oxides are the most widely used adsorbents in practical applications because of their high affinity for H_2S. However, their disadvantages of low surface areas and lack of pores lead to poor regeneration and reutilization. To solve these problems, many scholars have studied the desulfurization performance of metal oxides loaded on solid matrices. Kim *et al.* (2014) prepared carbon nanofiber webs loaded with ZnO through electrospinning, as presented in Fig. 3; the webs demonstrated a desulfurization ability that was three times greater than that of pure ZnO adsorbent. Sun *et al.* (2014a) used ferric oxides to modify the surface of AC and reported that the sulfur saturation capacity reached 50.1%. Wu *et al.* (2018) studied the H_2S removal property of a Zn-Al mixed metal oxide (Zn-Al-MMO) derived from layered double hydroxide in hot coal gas desulfurization. The adsorbent demonstrated an adequate sulfur capacity of 318.8 mg g^{-1}, and X-ray photoelectron spectroscopy (XPS) indicated the production of elemental sulfur during the desulfurization process, as shown in Fig. 4. Cimino *et al.* (2018) dispersed Zn and Cu oxides onto γ-Al_2O_3 and studied the desulfurization ability at room temperature; their experiments revealed that $Cu_{0.5}Zn_{0.5}/\gamma$-Al_2O_3 had the best adsorption capacity (27.9 mg g^{-1}) for H_2S under both dry and humid conditions.

MOF-based Functional Materials

MOFs are a type of porous crystalline materials consisting of a combination of organic ligands and metal ions or clusters. Because of their unique advantages of adjustable functionality, high porosity, and controllable composition, MOFs have attracted a considerable amount of attention in various fields, such as gas adsorption and catalysis. Hamon *et al.* (2011) compared the desulfurization performance of MIL-53(Cr) and MIL-47(V) at 30°C and discovered that the interactions of H_2S with both MIL-53(Cr) and MIL-47(V) were relatively weak and that the simulated adsorption enthalpies for H_2S were in decreasing order, MIL-53(Cr) (narrow pore) > MIL-47(V) > MIL-53(Cr) (large pore). Nickerl *et al.* (2014) investigated the H_2S removal ability

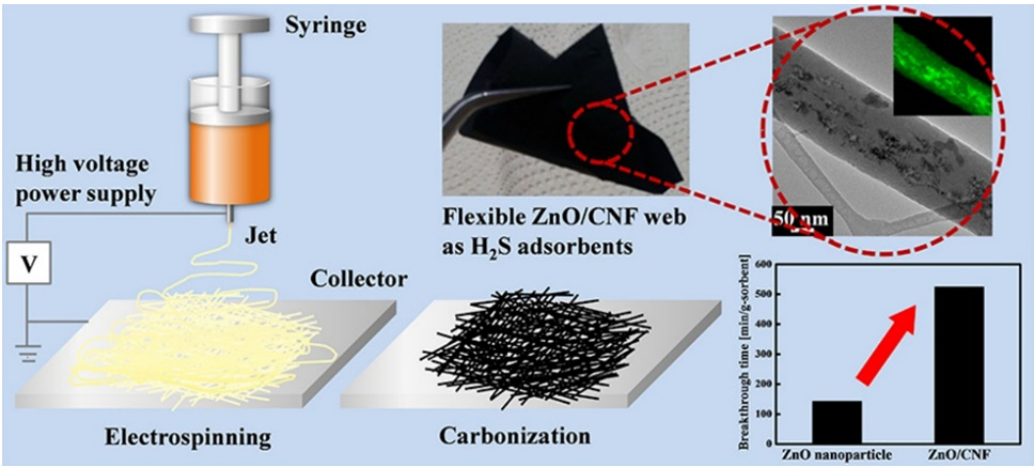

Fig. 3. A schematic of preparing ZnO/carbon nanofiber webs (Kim *et al.*, 2014).

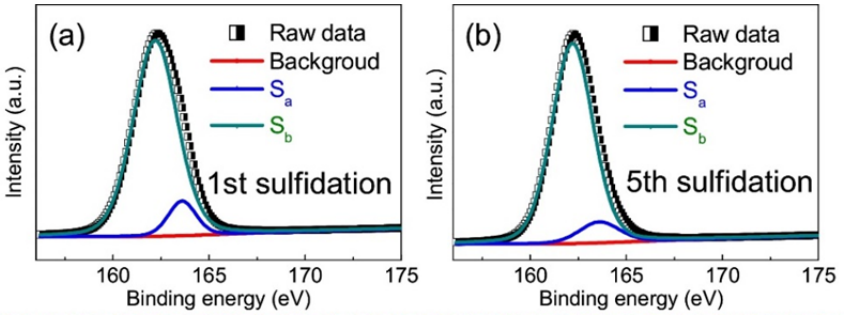

BEs and contents of different species obtained from XPS Spectra of S 2p

Samples	S_a		S_b	
	BE (eV)	Content (%)	BE (eV)	Content (%)
1st sulfidation	163.6	9.2	162.2	90.8
5th sulfidation	163.6	10.0	162.2	90.0

BE (Binding energy)

Fig. 4. Related results from S 2p XPS spectra of ZnAl-MMO (Wu *et al.*, 2018).

of metal salts (Cu^{2+}, Ni^{2+} and Co^{2+}) loaded on UiO-67; the adsorbent loaded with 86.8% $Cu(NO_3)_2$ had the highest H_2S capacity (7.8 wt.%). In addition, polyoxometalates (POMs) are widely used as catalysts in desulfurization because of their excellent redox ability. However, because pure POMs are solid materials and thus have low surface area, they do not exhibit ideal removal of H_2S, because of a poor utilization rate of activated sites. Therefore, some scholars have attempted to combine MOFs with POMs, using MOFs as support to improve the desulfurization and regeneration of POMs. Song *et al.* (2011) investigated a material that combined a Keggin-type POM ($[CuPW11O39]^{5-}$) with MOF-199 for H_2S removal. Solid octasulfur (S_8) was produced by using the composite, whereas pure MOF-199 did not produce S_8. Lange *et al.* (2015) also investigated the removal performance of the aforementioned composite material for H_2S and methyl parathion at room temperature. Demir *et al.* (2017) evaluated the selective H_2S adsorption of functionalized UiO-66 with a series of functional groups through computational methods. Al-Jadir and Siperstein (2018) assessed the selective H_2S/CH_4 adsorption of UiO-66, UiO-67, and UiO-68 to study the effects of the pore sizes of MOFs on H_2S removal. The result revealed that linkers had no obvious influence on macroscopic properties at low pressures, but the differences among linkers increased at high pressures. Analysis of the selective adsorption parameter revealed that UiO-67 had the greatest potential for separating H_2S from natural gas. Sánchez-González *et al.* (2018) prepared Mg-CUK-1 using water as the solvent for H_2S and CO_2 adsorption. An adsorption experiment demonstrated that the ecofriendly adsorbent could achieve reversible adsorption of H_2S; a regeneration experiment revealed that the adsorption performance could be maintained after multiple cycles, and long-range crystallinity could be retained during the regeneration process. Liu *et al.* (2017) investigated the selective separation of 11 MOFs for H_2S

and CO_2 reporting that Mg-MOF-74, MIL-101(Cr), UiO-66, ZIF-8, and Ce-BTC had completely reversible physical adsorption of H_2S; among them, MIL-101(Cr) exhibited the best separation performance for H_2S/CO_2. Liu *et al.* (2018a) reported a novel hybrid membrane, a rare earth, face-centered cubic-MOF (RE-fcu-MOF), modified by polymers, to remove H_2S and CO_2 from natural gas. Recently, Huang and Wang (2019) reported core-shell structure H_2S-imprinted polymers loaded on a polyoxometalate@Zr-based metal-organic framework using water as a substitution template to achieve the selective removal of H_2S from gases containing CO_2. They found that this functional adsorbent had excellent separation for H_2S/CO_2, and could transform H_2S to sulphur. The results suggested that the adsorbent had excellent selectivity and desulfurization properties.

Nitrogen Oxides

NO_x compounds are the products of reactions between nitrogen and oxygen in high-temperature combustion processes, such as those associated with internal combustion engine exhaust and power station boilers. NO_x is a general term for all nitrogen oxides, including nitric oxide (NO) and nitrogen dioxide (NO_2), which belong to a type of air pollutants that can cause smog and acid rain (Hu *et al.*, 2019). In addition, NO_x can react with ammonia, moisture, and other compounds to produce nitric acid, which causes considerable harm to lung tissue. Thus, the OSHA stipulated that the permissible exposure levels of NO and NO_2 were 25 and 5 ppm, respectively (Decoste and Peterson, 2014). Current NO_x removal methods mainly include adsorption, absorption, catalytic decomposition, and selective catalytic reduction (Jiang *et al.*, 2018). Adsorption has been widely studied for NO_x removal because of its advantages of a relatively high removal rate, no secondary pollution, and no energy loss. Therefore, various functional adsorbents, including MOF-based, carbon-based, zeolite-based, and composite materials (listed in Table 3), have been proposed to achieve highly effective removal of NO.

Carbon-based Functional Materials

Belhachemi *et al.* (2014) compared the NO_2 adsorption capacities of different ACs, which were prepared through physical and chemical activation of date pits or obtained through the modification of commercialized AC. The

Table 3. Functional adsorbents for NO_x removal.

Adsorbents	NO_2 (mg g^{-1})	NO (mg g^{-1})	composition	Ref.
AC	39		NO_2 in N_2	Yu *et al.* (2018)
C_{CO2}	129			
C_{Zn}	124			
GAC	127			
GAC-O	78			
GAC-O-T	136			
Ordered mesoporous carbon (OMC)		16.35	NO, O_2 in Ar	Ebrahim *et al.* (2014)
Ce-OMC		18.61		
AC from sawdust	54.7		NO_2 in N_2	Choi *et al.* (2014)
AC		11.3	NO, O_2 in Ar	Mendt *et al.* (2017)
Cu/AC		42.39	NO, O_2 in N_2	Zhao *et al.* (2017)
Zn/AC		34.23		
M5AC7	16.3		0.1 % of NO_2	Chen *et al.* (2014)
M7AC7	13.4			
M5AC8	12.0			
M7AC8	29.2			
A-N_2-D-N_2		11.1	NO, O_2 in N_2	Severa *et al.* (2015)
A-O_2-D-N_2		11.4		
A-N_2-O_2-D-N_2		11.4		
UiO-66 (dry)	73		NO_2 in N_2	Babu *et al.* (2016)
UiO-66 (moist)	40			
UiO-67 (dry)	79			
UiO-67 (moist)	118			
Urea/UiO-66 (dry)	37		NO_2 in N_2	Sun *et al.* (2016)
Urea/UiO-66 (moist)	101			
Melamine/UiO-66 (dry)	3			
Melamine/UiO-66 (moist)	10			
Urea/UiO-67 (dry)	74			
Urea/UiO-67 (moist)	154			
Melamine/UiO-67 (dry)	41			
Melamine/UiO-67 (moist)	93			
MIPa (AA as functional monomers)		0.121	NO in N_2	Iberahim *et al.* (2018)
MIPb (AAM as functional monomers)		0.112		

results demonstrated that the AC from date pits had a high NO_2 adsorption capacity (129 mg g^{-1}) similar to that of commercialized adsorbents. They also discovered that the presence of strong acidic groups such as carboxylic acids, anhydrides, and lactones inhibited the reduction of NO_2 into NO. Wang *et al.* (2014) prepared AC fibers loaded with manganese dioxide (MnO_2) and studied the effect of the amount of MnO_2 loading on the NO removal efficiency at room temperature. They found that appropriate amounts of MnO_2 can improve the NO removal efficiency of AC; moreover, the oxidation efficiency of NO reached 30.6% when the amount of MnO_2 was 3.64 wt%. Saputro *et al.* (2017) investigated the selectivity adsorption of the ZnO (0002) surface for NO and carbon monoxide by performing density functional theory (DFT) calculations. They found that a clean ZnO (0002) surface exhibited better selectivity for NO than for CO. Sager *et al.* (2016) studied the NO_2 separation of AC modified with copper oxide (CuO)/ZnO at an ambient temperature; when the loading amount of CuO/ZnO was 20 wt%, CuO/ZnO-AC demonstrated excellent removal ability for NO_2. Bazan *et al.* (2016) prepared AC under different carbonization and activation temperatures to analyze the effects of these two factors on NO_2 removal. Under dry conditions, AC that was prepared using carbonization and activation temperatures of 700°C and 800°C, respectively, had the best NO_2 adsorption capacity of 29.2 mg g^{-1}. However, AC that was prepared using carbonization and activation temperatures of 500°C and 700°C, respectively, exhibited the best removal capacity of 102.1 mg g^{-1} under mix-dry conditions. Guo *et al.* (2018) conducted the first study that used DFT to investigate the NO and NO_2 adsorption behavior of pristine and B-atom-embedded γ-graphene. B-atom-embedded γ-graphene had stronger chemical interactions with NO and NO_2 than pristine γ-graphene.

Zeolite-based Functional Materials

Sun *et al.* (2014b) compared the performance of 12 porous materials as adsorbents for removing NO_x from flue gases; these materials comprised four all-silica zeolites, six MOFs, and two zeolitic imidazolate frameworks (ZIFs). The results indicated that Cu-BTC had the best adsorption of NO_x, and the other adsorbents could not provide effective separation with large adsorption capacities for NO_x; this shortcoming was attributed to the small dipole moment of NO_x. Skarlis *et al.* (2014) investigated the storage of NO_x on Fe-BEA zeolite through Fourier transform infrared spectroscopy. Liu *et al.* (2015b) proposed a novel and ultrafast method to prepare high-silica zeolite SSZ-13 in 10 min. After copper ion exchange, the prepared SSZ-13 exhibited excellent removal of NO_x. Pan *et al.* (2015) studied the NO_x adsorption of Fe/zeolites in the presence of SO_2, CO_2 and water (H_2O). The results revealed the NO_x adsorption capacities of the Fe/zeolite, which in descending order were as follows: Fe/MOR > Fe/FER > Fe/ZSM-5 > Fe/Beta; moreover, the adsorption capacity of Fe/MOR for NO_x was approximately 3.2 mg g^{-1}. In the presence of 100-ppm SO_2, 10% CO_2, and 10% H_2O, the adsorption capacity of Fe/MOR for NO_x decreased to approximately 2.0 mg g^{-1}. Yu *et al.* (2018b) investigated the NO removal of HZSM-5 from flue gas through adsorption-plasma processes, including A-N_2-D-N_2 (adsorption-N_2 flushing-nonthermal plasma decomposition-N_2 flushing), A-O_2-D-N_2 and A-N_2-O_2-D-N_2.

MOF-based Functional Materials

Ebrahim *et al.* (2012) studied the NO_2 adsorption properties of UiO-66 and UiO-67 at ambient temperatures. An experiment comparing UiO-66 and UiO-67 indicated that the size and chemistry of a ligand influenced the adsorption property. In addition, UiO-66 demonstrated a more favorable adsorption capacity in dry conditions than in moist conditions, suggesting that water has a negative effect on NO_2 adsorption. By contrast, the adsorption capacity of UiO-67 was higher under moist conditions than under dry conditions. On the basis of relevant research, the group utilized urea and melamine with NH_2 groups to modify UiO-66 and UiO-67 and thus be capable of effectively removing NO_2 under either dry or moist conditions. A series of experiments revealed that the adsorption capacity of every adsorbent was higher under moist conditions than under dry conditions. The adsorption capacities of both UiO-66 and UiO-67 modified with urea exhibited obvious increases compared with pure UiO-66 and UiO-67 under moist conditions. However, the introduction of melamine negatively affected the adsorption performance of UiO-66 and UiO-67 for NO_2 (Ebrahim *et al.*, 2014). Mendt *et al.* (2017) investigated the NO adsorption of MIL-100 (Al) at low temperatures by employing pulsed electron paramagnetic resonance spectroscopy and DFT calculations.

Composite Materials

Zhao *et al.* (2016) synthesized NO-MIPs by using methanoic acid as a dummy template because the solubility of NO is low in organic solvents under ambient conditions. In their study, they used acrylic acid (AA) and acryl amide (AAM) as functional monomers to prepare MIPa and MIPb, respectively. The results demonstrated that the NO adsorption ability of MIPa was superior to that of MIPb, suggesting that the acidic functional monomer AA is beneficial for improving NO adsorption capacity. Selectivity experiments revealed that O_2 had no influence on NO adsorption capacity; the introduction of CO_2 and SO_2 led to the decrease of NO adsorption capacity. On the basis of their previous study, the group prepared two groups of NO-MIPs using methanoic acid, acetic acid, and ethanedioic acid as templates and AA and AAM as functional monomers. They discovered that the adsorbents with different functional monomers and templates had different pore sizes and surface areas, resulting in variations in adsorption capacity (Zhao and Wang, 2017).

Sulfur Dioxide

SO_2 is a poisonous and colorless gas that is released mainly by the combustion of fossil fuel and waste incineration. SO_2 can react with water vapor, O_2, and other compounds to form acid rain. Moreover, it can cause the development of respiratory diseases and severely harm human organs such as stomachs, livers, and kidneys. SO_2

removal is key method for improving air quality and human health (Hussain and Luo, 2019). In the past few years, researchers have proposed novel functional adsorbents such as carbon-based, zeolite-based, MOF-based, and composite materials to remove SO_2, as indicated in Table 4.

Carbon-based Functional Materials

Peng *et al.* (2014) studied the selective adsorption ability of AC for SO_2 and the desorption behavior of AC under microwave radiation. The selectivity result indicated that the presence of other gases in flue gas reduced the adsorption capacity to 28.73 mg g^{-1} for SO_2. Yi *et al.* (2014) investigated the SO_2, NO and CO_2.removal abilities of coconut shell ACs modified with Cu, Ca, Mg, and Zn, respectively. They reported that the following order of SO_2 adsorption capacity of each adsorbent: Zn/AC < Cu/AC < Mg/AC < Ca/AC. Tailor *et al.* (2014) prepared a series of adsorbents, including PEI, and poly(propyleneimine) second and third generation ((PPI-G2 and PPI-G3, respectively) dendrimers supported on SBA-15 and MCM-41, and investigated the selective adsorption ability of each material for SO_2. In the presence of mixture gas of SO_2 and N_2, the MCM-41 loaded with PPI-G3 exhibited the best selectivity for SO_2/N_2 compared with the other adsorbents. In addition, the SO_2 adsorption of MCM-41 loaded with PPI-G3 or PEI increased considerably under 19% relative humidity. Chen *et al.* (2014) obtained N-doped ordered mesoporous carbon spheres (N-OMCs) with a surface area of 566 m^2 g^{-1} by using a soluble urea-phenol-formaldehyde resin as a precursor and triblock copolymer F127 as a soft template. The breakthrough time was 22.8 min, and the SO_2 adsorption capacity was 119.1 mg g^{-1}. The SO_2 adsorption capacity exhibited no obvious changes during seven cycle experiments, demonstrating that the adsorbent had stable adsorption. Zhang *et al.* (2015) investigated the SO_2 adsorption of modified graphene oxides by performing DFT calculations and discovered that hydroxyl groups on graphene oxides can not only improve SO_2 adsorption but also promote the oxidation of SO_2 to SO_3. To adsorb trace SO_2, Ling *et al.* (2015) utilized a one-pot fabrication method of a calcium oxide (CaO)-carbon foam adsorbent, as shown in Fig. 5; the adsorbent had a hierarchical porous structure and retained a stable structure even after five cycles.

Severa *et al.* (2015) prepared ionic liquids (ILs) supported on AC to study SO_2 adsorption. They discovered that ILs based on acetate and lactate imidazolium anions demonstrated favorable adsorption capacity for SO_2 compared with those based on sulfate and halide anions. Sun *et al.* (2016)

Table 4. Functional adsorbents for SO_2 removal.

Adsorbents	SO_2 (mg g^{-1})	Temperature (°C)	composition	Ref.
N-OMC	119.1	25	SO_2 in N_2	Song *et al.* (2014)
MnO_2	200	250	SO_2, CO_2, O_2 and H_2O	Savage *et al.* (2016)
	400	450		
GO	150	25	SO_2	Zhang *et al.* (2016)
Pure PC	12.2	25	SO_2 in N_2	Glomb *et al.* (2017)
4.25% NPC	24.2			
7.57% NPC	35.3			
10.2% NPC	48.3			
Macro and micro GO	190.1	20	SO_2	Elder *et al.* (2018)
POSB	10.04	400	SO_2 in N_2	Mon *et al.* (2018)
MDEA/AC after CO_2 activation	156.22	120	1% SO_2 in N_2	Carter *et al.* (2018)
PILs-xerogels	514	25	SO_2 in N_2	Xia *et al.* (2018)
Propyldiethanolamine/MCM-41	181.8	23	1% SO_2 in N_2	Khan *et al.* (2000)
	137	50		
Triethylolamine/SBA-15	146.3	25	SO_2 in N_2	Quijano *et al.* (2011)
MFM-300(In)	529.9	25	SO_2, CO_2 in N_2	Wang *et al.* (2017b)
MFM-601	787.2	25	SO_2	Zhou *et al.* (2018)

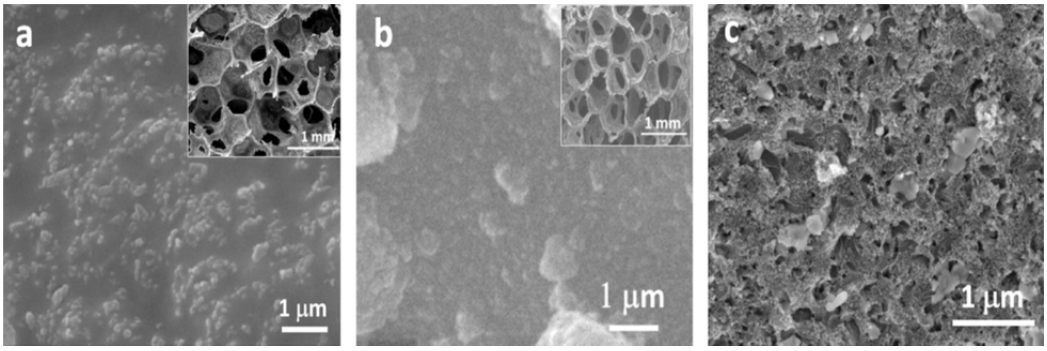

Fig. 5. SEM images of CaO/ carbon foam before heat treatment (a), before use (b) and after 5 cycles (c) (Ling *et al.*, 2015).

investigated how the amount of nitrogen loaded on the surface of NPCs affect SO_2 adsorption. The results demonstrated that the introduction of N can noticeably enhance the SO_2 adsorption capacity of porous carbon. On the basis of research on the use of palm oil mill sludge, Iberahim *et al.* (2018) prepared biochar through the pyrolysis method and studied its SO_2 adsorption ability. To further improve the SO_2 adsorption of AC, Shao *et al.* (2018b) used CO_2 activation and methyldiethanolamine (MDEA) impregnation to modify AC; the SO_2 adsorption capacity of AC increased from 57.78 to 156.22 mg g^{-1} after MDEA impregnation, demonstrating that MDEA impregnation treatment can effectively enhance the adsorption capacity of AC. Xia *et al.* (2018) designed a highly cross-linked nonporous poly(ionic liquid) xerogels through the polymerization of gemini ILs. Selectivity experiments demonstrated that the xerogels had no adsorption ability for CO_2, CH_4, or N_2, but the adsorption capacity for SO_2 reached 514 mg g^{-1}. The SO_2 adsorption capacity exhibited no remarkable changes after 50 cycle experiments. The results demonstrated that the prepared xerogels had remarkable adsorption performance for SO_2 and excellent regeneration ability.

MOF-based Functional Materials

Using the grand canonical Monte Carlo simulation method, Song *et al.* (2014) studied the SO_2 adsorption properties of MOFs with different pore sizes and topologies, including IRMOF-1, -8, -9, -10, and -15; MOF-177 and -505; Cu-BTC; MIL-47; and ZIF-8. The simulation results revealed that the MOFs with pore sizes larger than 0.4 nm exhibited excellent adsorption of SO_2. Savage *et al.* (2016) prepared porous MOF (MFM-300 (In)) and studied the selective adsorption of SO_2 with interference of CO_2, CH_4, and N_2 individually. The results demonstrated that MFM-300 (In) had a high SO_2 adsorption capacity of 529.9 mg g^{-1} and favorable selectivity for SO_2/CO_2 (60), SO_2/CH_4 (425), and SO_2/N_2 (5000) under ambient conditions. Mounfield *et al.* (2016) studied the adsorption performance of MIL-125 and MIL-125-NH_2 for SO_2 at 2.7 bar and found that the adsorption capacities were 10.9 and 10.3 mmol g^{-1}, respectively. In addition, they discovered that MIL-125-NH_2 can retain a stable structure under dry, humid, and aqueous SO_2 conditions. However, MIL-125 degraded when exposed to humid and aqueous SO_2, indicating that its stability requires improvement. Considering that ZIFs demonstrate favorable stability with respect to temperature and humidity, Bhattacharyya *et al.* (2016) studied the adsorption performance of ZIF-8 for SO_2 and analyzed its stability under dry, humid, and aqueous SO_2 conditions. The SO_2 saturation capacity was approximately 518.4 mg g^{-1} at 25°C and 2.5 bar in a dry environment. Characterization revealed that dry SO_2 had no influence on the stability of ZIF-8 at room temperature, humid SO_2 attacked the structure of ZIF-8, and ZIF-8 exhibited no structural degradation under aqueous SO_2 conditions. Ranjbar and Taher (2016) studied the adsorption property of Ni-MOF-74 for SO_2 at 25°C under the pressure range of 0 to 4 bar. The SO_2 adsorption capacity of Ni-MOF-74 increased in with the pressure, and the maximum capacity of 105.06 mmol g^{-1} was reached at 4 bar. Zhang *et al.* (2016) compared the SO_2 adsorption capacities of four MOFs loaded with polyacrylonitrile (PAN)—PAN/ZIF-8, PAN/Mg-MOF-74, PAN/MOF-199, PAN/UiO-66-NH_2—and reported that the PAN supported by the four MOFs had an adsorption ability that was superior to that of pure PAN; moreover, PAN/UiO-66-NH_2 exhibited the highest adsorption capacity of approximately 11 mg g^{-1} at 25°C. Glomb *et al.* (2017) prepared four dicarboxylate modified MOFs for SO_2 adsorption: 3D-[$Zn_4(\mu_4\text{-}O)(L1)_3$], 2D-[$Zn_2(L1)_2(DEF)_2 \cdot 2.5DEF$], [$Zn_2(L1)_2$(bipy)] and [$Zn_2(L1)_2$(bpe)]. Among them, [$Zn_2(L1)_2$(bipy)] exhibited the highest SO_2 adsorption capacity of 10.9 mmol g^{-1} at 293 K and 1 bar. Elder *et al.* (2018) investigated the adsorption performance of copper benzenedicarboxylate (CuBDC), zinc benzenedicarboxylate (ZnBDC) and cobalt benzenedicarboxylate (CoBDC) for humid SO_2; 88% of the SO_2 was adsorbed by CuBDC in a reduced oxidation state. Moreover, the structures of ZnBDC and CoBDC underwent changes when exposed to SO_2; this indicated that they were unsuitable for application in SO_2 removal. Mon *et al.* (2018) proposed a novel 3D MOF with hydrated barium cations for selective adsorption of SO_2, and the SO_2 adsorption capacity reached 2.5 mmol g^{-1} at 303 K and 0.025 bar. Carter *et al.* (2018) reported that a novel MFM-601 had a record-high SO_2 adsorption capacity of 12.3 mmol g^{-1} at 298 K and 1.0 bar; furthermore, the adsorbent exhibited fully reversible and highly selective adsorption for SO_2 with respect to CO_2 and N_2.

Cui *et al.* (2017) designed an inorganic anion-pillared hybrid porous adsorbent (silicon hexafluoride, SiF_6^{-2}) to achieve the efficient capture of SO_2; a high SO_2 adsorption capacity of 704.6 mg g^{-1} was reached at 1.01 bar, and an excellent SO_2/CO_2 selectivity of 89% was achieved at a low pressure (0.002 bar).

Volatile Organic Compounds

VOCs are a type of common air pollutant emitted through production in chemical, petrochemical, and related industries; some examples of these pollutants are benzene, toluene, hexane, CH_4 and sulfur compounds (Khan and Ghoshal, 2000). Deng *et al.* (2018) analyzed 36 VOCs from Longchuan Tunnel, Hefei, in eastern China, to study the atmospheric VOC pollution in urban areas of China. They found that alkanes (mainly branched alkanes) accounted for the largest proportion of 52%, and benzene homologues took the second place. These gases cause serious harm to the environment and human health, including by causing nausea, exposing humans to carcinogens, and contributing to global warming (Quijano *et al.*, 2011). Therefore, many absorbents and catalysts have been developed for the removal of VOCs. For example, some researchers have investigated the potential of using ILs as absorbents for VOC removal (Park *et al.*, 2017; Wang *et al.*, 2017a). Quijano *et al.* (2011) assessed the feasibility of using imidazole ILs for VOC removal in a multiphase bioreactor. The results suggested that the acclimation of VOCs by microorganisms alone was insufficient for achieving effective biodegradation in heterogeneous systems such as nonaqueous-phase ILs.

Wang *et al.* (2017b) investigated the adsorption potential of a [Bmim] [NTf2] absorbent for toluene. The solubility of toluene in [Bmim] [NTf2] was 61.5% at 20°C and standard atmospheric pressure. The maximum adsorption rate of toluene for [Bmim] [NTf2] was 98.3%. At a concentration of 300 ppm and flow rate of 50 mL min^{-1}, the adsorption rate of toluene could exceed 94% at 20°C. The results indicated that [Bmim] [NTf2] absorbents can remove toluene easily. Biard *et al.* (2018) simulated the countercurrent adsorption of four hydrophobic VOCs and two heavy organic solvents, namely polydimethylsioxane (PDMS) 50 and di-(2-ethylhexyl) adipate (DEHA), using fixed volume packed columns. VOC biodegradation experiments revealed that 5% (v v^{-1}) IL was toxic to activated sludge organisms, and the combination of IL and VOC may produce a synergistic toxic effect. After the domestication of target VOCs, only toluene biodegradability increased significantly in response to IL. The results revealed that ILs could strongly inhibit microbial activity in the presence of VOCs for more than 24 hours. Mo *et al.* (2019) reported that photocatalytic oxidation is a promising method for the removal of VOCs and reviewed the purification status of VOCs in indoor air. Park *et al.* (2017) investigated several strategies for removing VOCs from the atmosphere. VOCs could be effectively captured using activated carbon fiber (ACF) and mesoporous silica with high surface areas. Biard *et al.* (2016) utilized a simple dynamic adsorption method to evaluate the mass transfer performance of solvents for selective removal of VOCs. Four hydrophobic VOCs (toluene, acetone, dichloromethane, and isopropanol) were absorbed by water and two heavy organic solvents, namely DEHA and PDMS. The water had high selectivity, and the two organic solvents, especially DEHA, demonstrated strong binding affinity for all VOCs.

Fang *et al.* (2016) prepared a series of new paraffin/surfactant/water emulsion (PSW) materials, and studied their potential for VOC removal. PSW-5 (5%, v v^{-1}) had higher adsorption efficiency for toluene than did other absorbents. The absorptivity of PSW-5 towards toluene reached 82.42%, and it remained 82.42% after three cycles. Yu *et al.* (2018a) selected benzene, toluene and xylene (BTX) as VOC representatives to measure the vapor-liquid equilibrium of BTX+ [EMIM] [Tf2N] mixtures. Cardoso *et al.* (2008) prepared ACs using cork powder waste as the raw material, and studied the adsorption potential of ACs for VOCs. Three ACs were prepared through the chemical activation of cork powder waste with KOH as the activator. The adsorbent had a large surface area exceeding 1300 m^2 g^{-1} and a micropore volume greater than 0.5 cm^3 g^{-1}. They discovered that the adsorbent at the highest activation temperature and KOH dosage exhibited the best removal and selective adsorption performance for VOCs.

Wang *et al.* (2016) developed hydrophobic functionalized SBA-15 through synthesis and post-modification of trimethylchlorosilane (TMCS) to remove VOCs. The adsorption and desorption properties of SBA-15-TMCS under various static and dynamic conditions were studied. The designed SBA-15-TMCS had high VOC adsorption capacity and recycling capacity. Zhou *et al.* (2018a) studied the effect of membrane adsorption on VOC recovery from oil and gas. The removal rate of heat-conducting oil absorbent was 86.50%, and that of an AbsFOV-97 absorbent was 90.44%. The performance of ABFOV-97 was superior to that of the heat-conducting oil. Moreover, a lower gas flow rate led to higher recovery from oil and gas. When the gas flow rate was less than 50 mL min^{-1}, the hydrocarbon removal rate was approximately 99.50%.

In addition, Iuga *et al.* (2011) used pyridine as the target molecules and MAA as the functional monomers to form a specific MIP, which demonstrated had strong selectivity for pyridine in the presence of toluene and benzene.

SUMMARY

In conclusion, the adsorption and regeneration properties of adsorbents require improvement in terms of working adsorption capacity, cycle life, and stability. To obtain a techno-economic system, the development of a new type of highly efficient adsorbent is necessary. In addition, few studies have been conducted in recent years on MIPs in the field of gas separation and removal, especially that of H_2S, SO_2, and NO_x. Therefore, designing functional adsorbents with excellent selectivity, adsorption and regeneration properties should be the focus of future research.

ACKNOWLEDGMENTS

This work was supported by the National Natural Science Foundation of China [Nos: 21276144, 21511130021], the Key Research and Development Program of Shandong Province, China [2017GSF217006], and Foundation of State Key Laboratory of High-efficiency Utilization of Coal and Green Chemical Engineering [No: 2017-K30].

REFERENCES

Abdullah, A.H., Mat, R., Somderam, S.A., Aziz, S.A. and Mohamed, A. (2018). Hydrogen sulfide adsorption by zinc oxide-impregnated zeolite (synthesized from Malaysian kaolin) for biogas desulfurization. *J. Ind. Eng. Chem.* 65: 334–342.

Akinyele, D.O. and Rayudu, R.K. (2014). Review of energy storage technologies for sustainable power networks. *Sustainable Energy Technol. Assess.* 8: 74–91.

Al-Jadir, T.M. and Siperstein, F.R. (2018). The influence of the pore size in Metal-Organic Frameworks in adsorption and separation of hydrogen sulphide: A molecular simulation study. *Microporous Mesoporous Mater.* 271: 160–168.

An, H., Feng, B. and Su, S. (2009). CO_2 capture by electrothermal swing adsorption with activated carbon fibre materials. *Carbon* 47: 2396–2405.

Asad, M. and Sheikhi, M.H. (2014). Surface acoustic wave based H_2S gas sensors incorporating sensitive layers of single wall carbon nanotubes decorated with Cu nanoparticles. *Sens. Actuators, B* 198: 134–141.

Babu, D.J., Kühl, F.G., Yadav, S., Markert, D., Bruns, M.,

Hampe, M.J. and Schneider, J.J. (2016). Adsorption of pure SO_2 on nanoscaled graphene oxide. *RSC Adv.* 6: 36834–36839.

Balsamo, M., Cimino, S., De Falco, G., Erto, A. and Lisi, L. (2016). ZnO-CuO supported on activated carbon for H_2S removal at room temperature. *Chem. Eng. J.* 304: 399–407.

Barelli, L., Bidini, G., Micoli, L., Sisani, E. and Turco, M. (2018). 13X Ex-Cu zeolite performance characterization towards H_2S removal for biogas use in molten carbonate fuel cells. *Energy* 160: 44–53.

Bazan, A., Nowicki, P. and Pietrzak, R. (2016). Removal of NO_2 by carbonaceous adsorbents obtained from residue after supercritical extraction of marigold. *Adsorption* 22: 465–471.

Beidari, M., Lin, S. and Lewis, C. (2017). Multiplier effects of energy consumption and CO_2 emissions by input-output analysis in South Africa. *Aerosol Air Qual. Res.* 17: 1666–1678.

Belhachemi, M., Jeguirim, M., Limousy, L., Addoun, F. (2014). Comparison of NO_2 removal using date pits activated carbon and modified commercialized activated carbon via different preparation methods: Effect of porosity and surface chemistry. *Chem. Eng. J.* 253: 121–129.

Belmabkhout, Y., Serna-Guerrero, R. and Sayari, A. (2010) Microporous carbonaceous adsorbents for CO_2 separation via selective adsorption. *Chem. Eng. Sci.* 65: 3695–3698.

Bhatt, P.M., Belmabkhout, Y., Assen, A.H., Weseliński, Ł.J., Jiang, H., Cadiau, A., Xue, D. and Eddaoudi, M. (2017). Isoreticular rare earth fcu-MOFs for the selective removal of H_2S from CO_2 containing gases. *Chem. Eng. J.* 324: 392–396.

Bhattacharyya, S., Pang, S.H., Dutzer, M.R., Lively, R.P., Walton, K.S., Sholl, D.S. and Nair, S. (2016). Interactions of SO_2-containing acid gases with ZIF-8: structural changes and mechanistic investigations. *J. Phys. Chem. C* 120: 27221–27229.

Biard, P., Coudon, A., Couvert, A. and Giraudet, S. (2016). A simple and timesaving method for the mass-transfer assessment of solvents used in physical absorption. *Chem. Eng. J.* 290: 302–311.

Biard, P., Couvert, A. and Giraudet, S. (2018). Volatile organic compounds adsorption in packed column: Theoretical assessment of water, DEHA and PDMS50 as absorbents. *J. Ind. Eng. Chem.* 59: 70–78.

Boysen, R. (2018). Advances in the development of molecularly imprinted polymers for the separation and analysis of proteins with liquid chromatography. *J. Sep. Sci.* 42: 51–71.

Cao, F., Chen, J., Ni, M., Song, H., Xiao, G., Wu, W., Gao, X. and Cen, K. (2014). Adsorption of NO on ordered mesoporous carbon and its improvement by cerium. *RSC Adv.* 4: 16281–16289.

Cara, C., Rombi, E., Musinu, A., Mameli, V., Ardu, A., Angotzi, M.S., Atzori, L., Niznansky, D., Xin, H.L. and Cannas, C. (2017). MCM-41 support for ultrasmall γ-Fe_2O_3 nanoparticles for H_2S removal. *J. Mater. Chem. A* 5: 21688–21698.

Cara, C., Rombi, E., Mameli, V., Ardu, A., Sanna Angotzi, M., Niznansky, D., Musinu, A. and Cannas, C. (2018). γ-Fe_2O_3-$M_{41}S$ sorbents for H_2S removal: Effect of different porous structures and silica wall thickness. *J. Phys. Chem. C* 122: 12231–12242.

Cardoso, B., Mestre, A., Carvalho, A. and Pires, J. (2008) Activated carbon derived from cork powder waste by KOH activation: preparation, characterization, and VOCs adsorption. *Ind. Eng. Chem. Res.* 47: 5841–5846.

Carter, J.H., Han, X., Moreau, F.Y., Silva, I. da, Nevin, A., Godfrey, H.G., Tang, C., Yang, S. and Schröder, M. (2018). Exceptional adsorption and binding of sulfur dioxide in a robust zirconium-based metal–organic framework. *J. Am. Chem. Soc.* 140: 15564–15567.

Chen, A., Yu, Y., Zhang, Y., Zang, W., Yu, Y., Zhang, Y., Shen, S. and Zhang, J. (2014). Aqueous-phase synthesis of nitrogen-doped ordered mesoporous carbon nanospheres as an efficient adsorbent for acidic gases. *Carbon* 80: 19–27.

Chen, C., Yang, S., Ahn, W., Ryoo, R. (2009). Amine-impregnated silica monolith with a hierarchical pore structure: Enhancement of CO_2 capture capacity. *Chem. Commun.* 24: 3627–3629.

Chen, C., Son, W., You, K., Ahn, J. and Ahn, W. (2010). Carbon dioxide capture using amine-impregnated HMS having textural mesoporosity. *Chem. Eng. J.* 161: 46–52.

Chen, X., Shen, B. and Sun, H. (2018a). Ion-exchange modified zeolites X for selective adsorption desulfurization from Claus tail gas: Experimental and computational investigations. *Microporous Mesoporous Mater.* 261: 227–236.

Chen, Y., Qiao, Z., Huang, J., Wu, H., Xiao, J., Xia, Q., Xi, H., Hu, J., Zhou, J. and Li, Z. (2018b). Unusual Moisture-enhanced CO_2 Capture within Microporous PCN-250 Frameworks. *ACS Appl. Mater. Interfaces* 44: 38638–38647.

Cheong, W., Yang, S. and Ali, F. (2013). Molecular imprinted polymers for separation science: A review of reviews. *J. Sep. Sci.* 36: 609–628.

Choi, S.J., Jang, B.H., Lee, S.J., Min, B.K., Rothschild, A. and Kim, I.D. (2014). Selective detection of acetone and hydrogen sulfide for the diagnosis of diabetes and halitosis using SnO_2 nanofibers functionalized with reduced graphene oxide nanosheets. *ACS Appl. Mater. Interfaces* 6: 2588–2597.

Chu, J., Wang, X., Wang, D., Yang, A., Lv, P., Wu, Y., Rong, M. and Gao, L. (2018). Highly selective detection of sulfur hexafluoride decomposition components H_2S and SOF_2 employing sensors based on tin oxide modified reduced graphene oxide. *Carbon* 135: 95–103.

Cimino, S., Lisi, L., de Falco, G., Montagnaro, F., Balsamo, M. and Erto, A. (2018). Highlighting the effect of the support during H_2S adsorption at low temperature over composite Zn-Cu sorbents. *Fuel* 221: 374–379.

Cui, X., Yang, Q., Yang, L., Krishna, R., Zhang, Z., Bao, Z., Wu, H., Ren, Q., Zhou, W., Chen, B. and Xing, H. (2017). Ultrahigh and selective SO_2 uptake in inorganic

anion-pillared hybrid porous materials. *Adv. Mater.* 29: 1606929.

DeCoste, J.B. and Peterson, G.W. (2014). Metal–organic frameworks for air purification of toxic chemicals. *Chem. Rev.* 114: 5695–5727.

Demir, H., Walton, K.S. and Sholl, D.S. (2017). Computational screening of functionalized UiO-66 materials for selective contaminant removal from air. *J. Phys. Chem. C* 121: 20396–20406.

Deng, C., Jin, Y., Zhang, M., Liu, X. and Yu, Z. (2018). Emission characteristics of VOCs from on-road vehicles in an urban tunnel in eastern China and predictions for 2017-2026. *Aerosol Air Qual. Res.* 18: 3025–3034.

Duong-Viet, C., Liu, Y., Ba, H., Truong-Phuoc, L., Baaziz, W., Nguyen-Dinh, L., Jean-Mario, N. and Pham-Huu, C. (2016). Carbon nanotubes containing oxygenated decorating defects as metal-free catalyst for selective oxidation of H_2S. *Appl. Catal. B* 191: 29–41.

Ebrahim, A.M., Levasseur, B. and Bandosz, T.J. (2012) Interactions of NO_2 with Zr-based MOF: effects of the size of organic linkers on NO_2 adsorption at ambient conditions. *Langmuir* 29: 168–174.

Ebrahim, A.M. and Bandosz, T.J. (2014). Effect of amine modification on the properties of zirconium–carboxylic acid based materials and their applications as NO_2 adsorbents at ambient conditions. *Microporous Mesoporous Mater.* 188: 149–162.

Elder, A.C., Bhattacharyya, S., Nair, S. and Orlando, T.M. (2018). Reactive adsorption of humid SO_2 on metal–organic framework nanosheets. *J. Phys. Chem. C* 122: 10413–10422.

Elsabawy, K. and Fallatah, A. (2019). Synthesis of newly wings like structure non-crystalline Niþþ-1,3,5-tribenzyl-1,3,5-triazine-2,4,6-(1H,3H,5H)-trione coordinated MOFs for CO_2 Capture. *J. Mol. Struct.* 1177: 255–259.

Elyassi, B., Al Wahedi, Y., Rajabbeigi, N., Kumar, P., Jeong, J.S., Zhang, X., Kumar, P., Balasubramanian, V., Katsiotis, M., Andre Mkhoyan, K., Boukos, N., Al Hashimi, S. and Tsapatsis, M. (2014). A high-performance adsorbent for hydrogen sulfide removal. *Microporous Mesoporous Mater.* 190: 152–155.

Fang, P., Tang, Z., Chen, X., Tang, Z., Chen, D., Huang, J., Zeng, W. and Cen, C. (2016). Experimental study on the adsorption of toluene from exhaust gas by paraffin/surfactant/water emulsion. *J. Chem.* 2016: 9385027.

Farooq, M., Almustapha, M.N., Imran, M., Saeed, M.A. and Andresen, J.M. (2018). In-situ regeneration of activated carbon with electric potential swing desorption (EPSD) for the H_2S removal from biogas. *Bioresour. Technol.* 249: 125–131.

Fauteux-Lefebvre, C., Abatzoglou, N., Blais, S., Braidy, N. and Hu, Y. (2015). Iron oxide-functionalized carbon nanofilaments for hydrogen sulfide adsorption: The multiple roles of carbon. *Carbon* 95: 794–801.

Gholidoust, Maina, J., Merenda, A., Schütz, J., Kong, L., Hashisho, Z. and Dumée, L. (2019). CO_2 sponge from plasma enhanced seeded growth of metal organic frameworks across carbon nanotube bucky-papers. *Sep. Purif. Technol.* 209: 571–579.

Glomb, S., Woschko, D., Makhloufi, G. and Janiak, C. (2017). Metal–organic frameworks with internal urea-functionalized dicarboxylate linkers for SO_2 and NH_3 adsorption. *ACS Appl. Mater. Interfaces* 9: 37419–37434.

Gonçalves, D.V., Paiva, M.A., Oliveira, J.C., Bastos-Neto, M.S. and Lucena, M. (2018). Prediction of the monocomponent adsorption of H_2S and mixtures with CO_2 and CH_4 on activated carbons. *Colloids Surf. A* 559: 342–350.

Guo, Y., Chen, Z., Wu, W., Liu, Y. and Zhou, Z. (2018) Adsorption of NO_x (x=1, 2) gas molecule on pristine and B atom embedded γ-graphyne based on first-principles study. *Appl. Surf. Sci.* 455: 484–491.

Gupta, A.K., Ibrahim, S. and Shoaibi, A. (2016). Advances in sulfur chemistry for treatment of acid gases. *Prog. Energy Combust. Sci.* 54: 65–92.

Habeeb, O., Kanthasamy, R., Ali, G., Sethupathi, S., and Yunus, R. (2017). Hydrogen sulfide emission sources, regulations, and removal techniques: A review. *Rev. Chem. Eng.* 34: 837–854.

Hamon, L., Leclerc, H., Ghoufi, A., Oliviero, L., Travert, A., Lavalley, J.C., Devic, T., Serre, C., Ferey, G., Vimont, A. and Maurin, G. (2011). Molecular insight into the adsorption of H_2S in the flexible MIL-53 (Cr) and rigid MIL-47 (V) MOFs: infrared spectroscopy combined to molecular simulations. *J. Phys. Chem. C* 115: 2047–2056.

Hao, X., Hou, G., Zheng, P., Liu, R. and Liu, C. (2016). H_2S in-situ removal from biogas using a tubular zeolite/TiO_2 photocatalytic reactor and the improvement on methane production. *Chem. Eng. J.* 294: 105–110.

He, H., Zhuang, L., Chen, S. and Liu, H. (2016). A solid amine adsorbent prepared by molecularly imprinting and its CO_2 adsorption properties. *Chem. Asian J.* 11: 3055.

Hu, Y., Li, Z., Wang, Y., Wang, L., Zhu, H., Chen, L., Guo, X., An, C., Jiang, Y. and Liu, A. (2019). Emission factors of NO_x, SO_2, PM and VOCs in pharmaceuticals, brick and food industries in Shanxi, China. *Aerosol Air Qual. Res.* 19: 1785–1797.

Huang, Y. and Wang, R. (2018). Review on fundamentals, preparations and applications of imprinted polymers. *Curr. Org. Chem.* 22: 1600–1618.

Huang, Y. and Wang, R. (2019). Highly selective separation of H_2S and CO_2 using a H_2S-imprinted polymers loaded on a polyoxometalate@zr-based metal-organic framework with a core-shell structure at ambient temperature. *J. Mater. Chem. A* 7: 12105–12114.

Huang, Z.H., Liu, G. and Kang, F. (2012). Glucose-promoted Zn-based metal–organic framework/graphene oxide composites for hydrogen sulfide removal. *ACS Appl. Mater. Interfaces.* 4: 4942–4947.

Huang, Z.B., Liu, B.S., Wang, F. and Amin, R. (2015). Performance of Zn-Fe-Mn/MCM-48 sorbents for high temperature H_2S removal and analysis of regeneration process. *Appl. Surf. Sci.* 353: 1–10.

Hussain, R. and Luo, K. (2019). The geological availability and emissions of sulfur and SO_2 from the typical coal of China. *Aerosol Air Qual. Res.* 19: 559–570.

Iberahim, N., Sethupathi, S. and Bashir, M.J. (2018). Optimization of palm oil mill sludge biochar preparation for sulfur dioxide removal. *Environ. Sci. Pollut. Res.* 25: 25702–25714.

Iuga, C., Ortíz, E. and Noreña, L. (2011). Interaction between volatile organic compounds and functional monomers in molecularly imprinted materials. *Nanotech Conf. Expo.* 3: 777–780.

Jiang, J., Ye, B. and Liu, J. (2019). Research on the peak of CO_2 emissions in the developing world: Current progress and future prospect. *Appl. Energy* 235: 186–203.

Jiang, Y., Bao, C., Liu, S., Liang, G., Lu, M., Lai, C., Shi, W. and Ma, S. (2018). Enhanced activity of Nb-modified CeO_2/TiO_2 catalyst for the selective catalytic reduction of NO with NH_3. *Aerosol Air Qual. Res*. 18: 2121–2130.

Kazmierczak-Razna, J., Gralak-Podemska, B., Nowicki, P. and Pietrzak, R. (2015). The use of microwave radiation for obtaining activated carbons from sawdust and their potential application in removal of NO_2 and H_2S. *Chem. Eng. J.* 269: 352–358.

Khan, F., Ghoshal, A. and Loss, J. (2000). Removal of volatile organic compounds from polluted air. *Prev. Process Ind.* 13: 527–545.

Kim, S., Bajaj, B., Byun, C.K., Kwon, S.J., Joh, H.I., Yi, K.B. and Lee, S. (2014). Preparation of flexible zinc oxide/carbon nanofiber webs for mid-temperature desulfurization. *Appl. Surf. Sci.* 320: 218–224.

Kong, Z., Niu, Z., He, L., Chen, Q., Zhou, L., Cheng, Y. and Guan, Q. (2018). In situ analysis of the adsorption behaviors of CO_2 on the surface of MIL-91(Al). *New J. Chem.* 42: 16985.

Kooti, M., Pourreza, A. and Rashidi, A. (2018) Preparation of MIL-101-nanoporous carbon as a new type of nanoadsorbent for H_2S removal from gas stream. *J. Nat. Gas Sci. Eng.* 57: 331–338.

Lai, Q., Diao, Z., Kong, L., Adidharma, H. and Fan, M. (2018). Amine-impregnated silicic acid composite as an efficient adsorbent for CO_2 capture. *Appl. Energy* 223: 293–301.

Lange, L.E. and Obendorf, S.K. (2015). Functionalization of cotton fiber by partial etherification and self-assembly of polyoxometalate encapsulated in $Cu_3(BTC)_2$ metal–organic framework. *ACS Appl. Mater. Interfaces* 7: 3974–3980.

Lau, L.C., Nor, N.M., Lee, K.T. and Mohamed, A.R.J. (2015). Selection of better synthesis route of CeO_2/NaOH/PSAC for hydrogen sulphide removal from biogas. *Environ. Chem. Eng.* 3: 1522–1529.

Lee, S. and Park, S. (2015). A review on solid adsorbents for carbon dioxide capture. *J. Ind. Eng. Chem.* 23: 1–11.

Lee, S., Lee, T. and Kim, D. (2017). Adsorption of hydrogen sulfide from gas streams using the amorphous composite of α-FeOOH and activated carbon powder. *Ind. Eng. Chem. Res.* 56: 3116–3122.

Li, D., Zhou, J., Wang, Y., Tian, Y., Wei, L., Zhang, Z., Qiao, Y. and Li, J. (2019). Effects of activation temperature on densities and volumetric CO_2 adsorption performance of alkali-activated carbons. *Fuel* 238: 232–239.

Li, Y., Wang, L. J., Fan, H. L., Shangguan, J., Wang, H. and Mi, J. (2014). Removal of sulfur compounds by a copper-based metal organic framework under ambient conditions. *Energy Fuels* 29: 298–304.

Li, Y., Guo, Y., Zhu, T. and Ding, S. (2016). Adsorption and desorption of SO_2, NO and chlorobenzene on activated carbon. *J. Environ. Sci.* 43: 128–135.

Li, Z., Liu, Y., Wang, H., Tsai, C., Yang, X., Xing, Y., Zhang, C., Xiao, P. and Webley, P. (2018). A numerical modelling study of SO_2 adsorption on activated carbons with new rate equations. *Chem. Eng. J.* 353: 856–866.

Liao, T., Kou, L., Du, A., Chen, L., Cao, C. and Sun, Z. (2018). H_2S sensing and splitting on atom-functionalized carbon nanotubes: A theoretical study. *Adv. Theory Simul.* 1: 1700033.

Ling, Z., Wan, P., Yu, C., Xiao, N., Yang, J., Long, Y. and Qiu, J. (2015). One-pot to fabrication of calcium oxide/carbon foam composites for the adsorption of trace SO_2. *Chem. Eng. J.* 259: 894–899.

Liu, C., Zhang, R., Wei, S, Wang, J., Liu, Y., Li, M. and Liu, R. (2015a). Selective removal of H_2S from biogas using a regenerable hybrid TiO_2 /zeolite composite. *Fuel* 157: 183–190.

Liu, D., Zhou, W. and Wu, J. (2016). CeO_2–MnO_x/ZSM-5 sorbents for H2S removal at high temperature. *Chem. Eng. J.* 284: 862–871.

Liu, F., Kuang, Y., Wang, S., Chen, S. and Fu, W. (2018b). Preparation and characterization of molecularly imprinted solid amine adsorbent for CO_2 adsorption. *New J. Chem.* 42: 10016–10023.

Liu, G., Chernikova, V., Liu, Y., Zhang, K., Belmabkhout, Y., Shekhah, O., Zhang, C., Yi, S., Eddaoudi, M. and Koros, W.J. (2018a). Mixed matrix formulations with MOF molecular sieving for key energy-intensive separations. *Nat. Mater.* 17: 283–289.

Liu, J., Wei, Y., Li, P., Zhao, Y. and Zou, R. (2017). Selective H_2S/CO_2 separation by metal–organic frameworks based on chemical-physical adsorption. *J. Phys. Chem. C.* 121: 13249–13255.

Liu, X. and Wang, R. (2017a). An innovative approach to oxidative removal of hydrogen sulfide using the solution of peroxo heteropolyacid. *Aerosol Air Qual. Res.* 17: 1341–1346.

Liu, X. and Wang, R. (2017b). Effective removal of hydrogen sulfide using 4A molecular sieve zeolite synthesized from attapulgite. *J. Hazard. Mater.* 326: 157–164.

Liu, Y., Ghimire, P. and Jaroniec, M. (2019). Copper benzene-1, 3, 5-tricarboxylate (Cu-BTC) metal-organic framework (MOF) and porous carbon composites as efficient carbon dioxide adsorbents. *J. Colloid Interface Sci.* 535: 122–132.

Liu, Z., Wakihara, T., Oshima, K., Nishioka, D., Hotta, Y., Elangovan, S.P., Yanaba, Y., Yoshikawa, T., Chaikittisilp, W., Matsuo, T., Takewaki, T. and Okubo, T. (2015b). Widening synthesis bottlenecks: realization of ultrafast and continuous-flow synthesis of high-silica zeolite

SSZ-13 for NO_x removal. *Chem. Int. Ed.* 54: 5683–5687.

Louis, L., Olivier, S., Robert, D.K., Hamelers and H.V.M. (2018). Solvent-free CO_2 capture using menbrance capcaitive deionization. *Environ. Sci. Technol.* 52: 9478–9485.

Maghsoudi, H., Soltanieh, M., Bozorgzadeh, H. and Mohamadalizadeh, A. (2013). Adsorption isotherms and ideal selectivities of hydrogen sulfide and carbon dioxide over methane for the Si-CHA zeolite: Comparison of carbon dioxide and methane adsorption with the all-silica DD3R zeolite. *Adsorption* 19: 1045–1053.

Marszewska, J. and Jaroniec, M. (2017). Tailoring porosity in carbon spheres for fast carbon dioxide adsorption. *J. Colloid Interface Sci.* 487: 162–174.

Matsuguchi, M. and Uno, T. (2006). Molecular imprinting strategy for solvent molecules and its application for QCM-based VOC vapor sensing. *Sens. Actuators, B* 113: 94–99.

Mendt, M., Barth, B., Hartmann, M. and Pöppl, A. (2017). Low-temperature binding of NO adsorbed on MIL-100 (Al)-A case study for the application of high resolution pulsed EPR methods and DFT calculations. *J. Chem. Phys.* 147: 224701.

Mo, J., Zhang, Y., Xu, Q., Lamson, J. and Zhao, R. (2009). Photocatalytic purification of volatile organic compounds in indoor air: A literature review. *Atmos. Environ.* 43: 2229–2246.

Mon, M., Tiburcio, E., Ferrando-Soria, J., San Millán, R. G., Navarro, J.A., Armentano, D. and Pardo, E. (2018). A post-synthetic approach triggers selective and reversible sulphur dioxide adsorption on a metal–organic framework. *Chem. Commun.* 54: 9063–9066.

Mounfield III, W.P., Han, C., Pang, S.H., Tumuluri, U., Jiao, Y., Bhattacharyya, S., Dutzer, M., Nair, S., Wu, Z., Lively, R., Sholl, D.S. and Walton, K. (2016). Synergistic effects of water and SO_2 on degradation of MIL-125 in the presence of acid gases. *J. Phys. Chem. C* 120: 27230–27240.

Nabavi, S., Vladisavljević, G., Zhu, Y. and Manović, V. (2017). Synthesis of size-tunable CO_2-philic imprinted polymeric particles (MIPs) for low-pressure CO_2 capture using oil-in-oil suspension polymerization. *Environ. Sci. Technol.* 51: 11476–11483.

Nam, H., Wang, S. and Jeong, H. R. (2018). TMA and H_2S gas removals using metal loaded on rice husk activated carbon for indoor air purification. *Fuel* 213: 186–194.

Nguyen, H., Tran, Y., Nguyen, H., Nguyen, T., Felipe Gańdara, and Nguyen, P. (2018). A series of metal–organic frameworks for selective CO_2 capture and catalytic oxidative carboxylation of olefins. *Inorg. Chem.* 21: 13772–13782.

Nickerl, G., Leistner, M., Helten, S., Bon, V., Senkovska, I. and Kaskel, S. (2014). Integration of accessible secondary metal sites into MOFs for H_2S removal. *Inorg. Chem. Front.* 1: 325–330.

Nowicki, P., Skibiszewska, P. and Pietrzak, R. (2014). Hydrogen sulphide removal on carbonaceous adsorbents prepared from coffee industry waste materials. *Chem. Eng. J.* 248: 208–215.

Ogungbenro, A., Quang, D., Al-Ali, K., Vega, L. and Abu-Zahra, M. (2018). Physical synthesis and characterization of activated carbon from date seeds for CO_2 capture. *J. Environ. Chem. Eng.* 6: 4245–4252.

Osaka, Y., Kito, T., Kobayashi, N., Kurahara, S., Huang, H., Yuan, H. and He, Z. (2015). Removal of sulfur dioxide from diesel exhaust gases by using dry desulfurization MnO_2 filter. *Sep. Purif. Technol.* 150: 80–85.

OSHA (2015). General safety and health. 2015. http://www.osha.gov/SLTC/etools/oilandgas/general_safety /general_safety.html.

Pai, K.N., Baboolal, J.D., Sharp, D.A. and Rajendran, A. (2019). Evaluation of diamine-appended metal-organic frameworks for post-combustion CO_2 capture by vacuum swing adsorption. *Sep. Purif. Technol.* 211: 540–550.

Pan, H., Guo, Y. and Bi, H.T. (2015). NO_x adsorption and reduction with C_3H_6 over Fe/zeolite catalysts: Effect of catalyst support. *Chem. Eng. J.* 280: 66–73.

Park, E., Seo, H. and Kim, Y. (2017). Influence of humidity on the removal of volatile organic compounds using solid surfaces. *Catal. Today* 295: 3–13.

Peng, S.Y., Wang, J.H. and Ma, L.P. (2014). Sulfur dioxide was carried out by activated carbon adsorption in combination with microwave desorption in scene. *Adv. Mater. Res.* 1049–1050: 44–49.

Quijano, G., Couvert, A., Amrane, A., Darracq, G., Couriol, C., Cloirec, P., Paquin, L. and Carrié, D. (2011). Potential of ionic liquids for VOC adsorption and biodegradation in multiphase systems. *Chem. Eng. Sci.* 66: 2707–2712.

Ranjbar, M. and Taher, M.A. (2016). Preparation of Ni-metal organic framework-74 nanospheres by hydrothermal method for SO_2 gas adsorption. *J. Porous Mater.* 23: 1249–1254.

Rayer, A., Mobley, P., Soukri, M., Gohndrone, T., Tanthana, J., Zhou, J. and Lail, M. (2018). Adsorption rates of carbon dioxide in amines in hydrophilic and hydrophobic solvents. *Chem. Eng. J.* 348: 514–525.

Rezakazemi, M., Darabi, M., Soroush, E. and Mesbah, M. (2019) CO_2 adsorptionenhancement by water-based nanofluids of CNT and SiO_2 using hollow-fiber membrane contactor. *Sep. Purif. Technol.* 210: 920–926.

Saeedirad, R., Ganjali, S.T., Bazmi, M. and Rashidi, A. (2018). Effective mesoporous silica-ZIF-8 nano-adsorbents for adsorptive desulfurization of gas stream. *J. Taiwan Inst. Chem. Eng.* 82: 10–22.

Sager, U., Däuber, E., Bathen, D., Asbach, C., Schmidt, F., Tseng, J.C., Pommerin, A., Weidenthaler, C. and Schmidt, W. (2016). Influence of the degree of infiltration of modified activated carbons with CuO/ZnO on the separation of NO_2 at ambient temperatures. *Adsorpt. Sci. Technol.* 34: 307–319.

Sánchez-González, E., Mileo, P.G., Sagastuy-Breña, M., Álvarez, J.R., Reynolds, J.E., Villarreal, A., Gutiérrez-Alejandre, A., Ramírez, J., Balmaseda, J., González-Zamora, E., Maurin, G., Humphrey, S. and Ibarra, I. (2018). Highly reversible sorption of H_2S and CO_2 by an environmentally friendly Mg-based MOF. *J. Mater. Chem.* 6: 16900–16909.

Santiago, R., Lemus, J., Moreno, D., Moya, C., Larriba,

M., Alonso-Morales, N., Gilarranz, M.A., Rodríguez, J.J. and Palomar, J. (2018). From kinetics to equilibrium control in CO_2 capture columns using Encapsulated Ionic Liquids (ENILs). *Chem. Eng. J.* 348: 661–668.

Saputro, A.G., Agusta, M.K., Yuliarto, B., Dipojono, H.K., Rusydi, F. and Maezono, R. (2017). Selectivity of CO and NO adsorption on ZnO (0002) surfaces: A DFT investigation. *Appl. Surf. Sci.* 410: 373–382.

Savage, M., Cheng, Y., Easun, T.L., Eyley, J.E., Argent, S.P., Warren, S.P., Warren, M.R., Lewis, W., Murray, C., Tang, C., Frogley, M., Cinque, G., Sun, J., Rudic, S., Murden, R., Benham, M., Fitch, A., Blake, A., Ramirez-Cuesta, A., Yang, S. and Schroder, M. (2016). Selective adsorption of sulfur dioxide in a robust metal–organic framework material. *Adv. Mater.* 28: 8705–8711.

Severa, G., Bethune, K., Rocheleau, R. and Higgins, S. (2015). SO_2 sorption by activated carbon supported ionic liquids under simulated atmospheric conditions. *Chem. Eng. J.* 265: 249–258.

Sevilla, M. and Fuertes, A. (2012). CO_2 adsorption by activated templated carbons. *J. Colloid Interface Sci.* 366: 147–154.

Shah, M.S., Tsapatsis, M. and Siepmann, J.I. (2015). Monte carlo simulations probing the adsorptive separation of hydrogen sulfide/methane mixtures using all-silica zeolites. *Langmuir* 31: 12268–12278.

Shalini, S., Nandi, S., Justin, A., Maity, R. and Vaidhyanathan, R. (2018). Potential of ultramicroporous metal–organic frameworks in CO_2 clean-up. *Chem. Commun.* 54: 13472.

Shao, L., Sang, Y., Huang, J. and Liu, Y. (2018a). Triazine-based hyper-cross-linked polymers with inorganic-organic hybrid framework derived porous carbons for CO_2 capture. *Chem. Eng. J.* 353: 1–14.

Shao, J., Zhang, J., Zhang, X., Feng, Y., Zhang, H., Zhang, S. and Chen, H. (2018b). Enhance SO_2 adsorption performance of biochar modified by CO_2 activation and amine impregnation. *Fuel* 224: 138–146.

Shin, M., Shin, Y. and Shin, J. (2018). Cholesterol recognition system by molecular imprinting on self-assembled monolayer. *Colloids Surf. A.* 559: 365–371.

Sidek, M., Cheah, Y., Zulkefli, N., Yusuf, N., Isahak, W. and Masdar, M. (2019). Effect of impregnated activated carbon on carbon dioxide adsorption performance for biohydrogen purification. *Mater. Res. Express* 6: 015510.

Sigot, L., Ducom, G. and Germain, P. (2016a). Adsorption of hydrogen sulfide (H_2S) on zeolite (Z): Retention mechanism. *Chem. Eng. J.* 287: 47–53.

Sigot, L., Obis, M.F., Benbelkacem, H., Germain, P. and Ducom, G. (2016b). Comparing the performance of a 13X zeolite and an impregnated activated carbon for H_2S removal from biogas to fuel an SOFC: Influence of water. *Int. J. Hydrogen Energy* 41: 18533–18541.

Silva, C., Howarth, A., Rimoldi, M., Islamoglu, T., Rinaldi, A. and Hupp, J. (2018). Phosphonates meet metal-organic frameworks: Towards CO_2 adsorption. *Isr. J. Chem.* 58: 1164–1170.

Skarlis, S.A., Berthout, D., Nicolle, A., Dujardin, C. and Granger, P. (2014). Combined IR spectroscopy and kinetic modeling of NO_x storage and NO oxidation on Fe-BEA SCR catalysts. *Appl. Catal. B* 148: 446–465.

Song, J., Luo, Z., Britt, D.K., Furukawa, H., Yaghi, O.M., Hardcastle, K.I. and Hill, C.L. (2011). A multiunit catalyst with synergistic stability and reactivity: A polyoxometalate-metal organic framework for aerobic decontamination. *J. Am. Chem. Soc.* 133: 16839–16846.

Song, X.D., Wang, S., Hao, C. and Qiu, J.S. (2014). Investigation of SO_2 gas adsorption in metal–organic frameworks by molecular simulation. *Inorg. Chem. Commun.* 46: 277–281.

Song, Z., Wei, Z., Wang, B., Luo, Z., Xu, S., Zhang, W., Yu, H., Li, M., Huang, Z., Zang, J., Yi, F. and Liu, H. (2016). Sensitive room-temperature H_2S gas sensors employing SnO_2 quantum wire/reduced graphene oxide nanocomposites. *Chem. Mater.* 28: 1205–1212.

Sun, F., Gao, J., Liu, X., Yang, Y. and Wu, S. (2016). Controllable nitrogen introduction into porous carbon with porosity retaining for investigating nitrogen doping effect on SO_2 adsorption. *Chem. Eng. J.* 290: 116–124.

Sun, T., Shen, Y. and Jia, J. (2014a). Gas cleaning and hydrogen sulfide removal for COREX coal gas by sorption enhanced catalytic oxidation over recyclable activated carbon desulfurizer. *Environ. Sci. Technol.* 48: 2263–2272.

Sun, W., Lin, L.C., Peng, X. and Smit, B. (2014b). Computational screening of porous metal-organic frameworks and zeolites for the removal of SO_2 and NO_x from flue gases. *AIChE J.* 60: 2314–2323.

Sun, X., Ruan, H., Song, X., Sun, L., Li, K., Ning, P. and Wang, C. (2018). Research into the reaction process and the effect of reaction conditions on the simultaneous removal of H_2S, COS and CS_2 at low temperature. *RSC Adv.* 8: 6996–7004.

Tailor, R., Abboud, M. and Sayari, A. (2014). Supported polytertiary amines: Highly efficient and selective SO_2 adsorbents. *Environ. Sci. Technol.* 48: 2025–2034.

Tailor, R. and Sayari, A. (2016). Grafted propyldiethanolamine for selective removal of SO_2 in the presence of CO_2. *Chem. Eng. J.* 289: 142–149.

Tehrani, N., Alivand, M., Maklavany, Da., Rashidi, A., Samipoorgiri, M., Seif, A. and Yousefian, Z. (2019) Novel asphaltene-derived nanoporous carbon with N-S-rich micro-T mesoporous structure for superior gas adsorption: Experimental and DFT study. *Chem. Eng. J.* 358: 1126–1138.

Tobiesen, F., Haugen, G. and Hartono, A. (2018). A systematic procedure for process energy evaluation for post combustion CO_2 capture: case study of two novel strong bicarbonate-forming solvents. *Appl. Energy* 211: 161–173.

Tomadakis, M.M., Heck, H.H., Jubran, M.E. and Al-Harthi, K. (2011). Pressure-swing adsorption separation of H_2S from CO_2 with molecular sieves 4A, 5A, and 13X. *Sep. Sci. Technol.* 46: 428–433.

Tran, H.L., Kuo, M.S., Yang, W.D. and Huang, Y.C. (2016). Hydrogen sulfide adsorption by thermally treated cobalt (II)-exchanged NaX zeolite. *Adsorpt. Sci. Technol.* 34: 275–286.

Wang, F., Yi, H. and Tang, X. (2017a). Removal of NO using a dielectric barrier discharge reactor in a cycled adsorption–desorption and decomposition system. *Arabian J. Sci. Eng.* 42: 1463–1474.

Wang, H., Wang, T., Han, L., Tang, M., Zhong, J., Huang, W. and Chen, R. (2016) VOC adsorption and desorption behavior of hydrophobic, functionalized SBA-15. *J. Mater. Res.* 31: 516–525.

Wang, M., Liu, H., Huang, Z.H. and Kang, F. (2014) Activated carbon fibers loaded with MnO_2 for removing NO at room temperature. *Chem. Eng. J.* 256: 101–106.

Wang, W., Ma, X., Grimes, S., Cai, H. and Zhang, M. (2017b). Study on the absorbability, regeneration characteristics and thermal stability of ionic liquids for VOCs removal. *Chem. Eng. J.* 328: 353–359.

Wang, X., Li, H., Liu, H., Hou, X. (2011). AS-synthesized mesoporous silica MSU-1 modified with tetraethylenepentamine for CO_2 adsorption. *Microporous Mesoporous Mater.* 142: 564–569.

Wang, Y., Wang, J., Ma, C., Qiao, W. and Ling, L. (2019). Fabrication of hierarchical carbon nanosheet-based networks for physical and chemical adsorption of CO_2. *J. Colloid Interface Sci.* 534: 72–80.

Wawrzyńczak, D., Majchrzak-Kucęba, I., Srokosz, K., Kozak, M., Nowak, W., Zdeb, J., Smółka, W. and Zajchowski, A. (2019). The pilot dual-reflux vacuum pressure swing adsorption unit for CO_2 capture from flue gas. *Sep. Purif. Technol.* 209: 560–570.

Wei, L., Gao, Z. and Wang, Y. (2017). Integrated two-stage adsorption for selective removal of CO_2 and SO_2 by amine-functionalized SBA-15. *Asia-Pacific J. Chem. Eng.* 12: 660–670.

Wu, M., Chang, B., Lim, T.T., Oh, W.D., Lei, J. and Mi, J. (2018). High-sulfur capacity and regenerable Zn-based sorbents derived from layered double hydroxide for hot coal gas desulfurization. *J. Hazard. Mater.* 360: 391–401.

Xia, L., Cui, Q., Suo, X., Li, Y., Cui, X., Yang, Q., Xu, J., Yang, Y. and Xing, H. (2018). Efficient, selective, and reversible SO_2 capture with highly crosslinked ionic microgels via a selective swelling mechanism. *Adv. Funct. Mater.* 28: 1704292.

Xie, W., Yu, M. and Wang, R. (2017). CO_2 capture behaviors of amine-modified resorcinol-based carbon aerogels adsorbents. *Aerosol Air Qual. Res.* 17: 2715–2725.

Xu, X., Cao, X., Zhao, L. and Sun, T. (2014). Comparison of sewage sludge-and pig manure-derived biochars for hydrogen sulfide removal. *Chemosphere* 111: 296–303.

Xu, Z., Deng, P., Li, J., Tang, S. and Cui, Y. (2019). Modification of mesoporous silica with molecular imprinting technology: A facile strategy for achieving rapid and specific adsorption. *Mater. Sci. Eng. C* 94: 684–693.

Yang, N. and Wang, R. (2015). Sustainable technologies for the reclamation of greenhouse gas CO_2. *J. Clean. Prod.* 103: 784–792.

Yi, H., Zuo, Y., Liu, H., Tang, X. Zhao, S., Wang, Z., Gao, F. and Zhang, B. (2014). Simultaneous removal of SO_2, NO, and CO_2 on metal-modified coconut shell activated carbon. *Water, Air, Soil Pollut.* 225: 1965.

Ying, W. and Nan, L. (2010). Molecular imprinting technology and its application. *Chem. Ind. Eng. Prog.* 29: 2315–2323.

Yu, G., Dai, C., Gao, H., Zhu, R., Du, X. and Lei, Z. (2018a). Capturing condensable gases with ionic liquids. *Ind. Eng. Chem. Res.* 57: 12202–12214.

Yu, Q., Gao, Y., Tang, X., Yi, H., Zhang, R. Zhao, S., Gao, F. and Zhou, Y. (2018b). Removal of NO from flue gas over HZSM-5 by a cycling adsorption-plasma process. *Catal. Commun.* 110: 18–22.

Yu, Z., Wang, X., Song, X., Liu, Y. and Qiu, J. (2015). Molten salt synthesis of nitrogen-doped porous carbons for hydrogen sulfide adsorptive removal. *Carbon* 95: 852–860.

Yun, S., Lee, H., Lee, W.E. and Park, H.S. (2016). Multiscale textured, ultralight graphene monoliths for enhanced CO_2 and SO_2 adsorption capacity. *Fuel* 174: 36–42.

Zha, Y., Shen, Y., Bai, L., Hao, R. and Dong, L. (2012). Synthesis and CO_2 adsorption properties of molecularly imprinted adsorbents. *Environ. Sci. Technol.* 46: 1789–1795.

Zhang, G., Sun, Y., Xu, Y. and Zhang, R. (2018). Catalytic performance of N-doped activated carbon supported cobalt catalyst for carbon dioxide reforming of methane to synthesis gas. *J. Taiwan Inst. Chem. Eng.* 93: 234–244.

Zhang, H., Cen, W., Liu, J., Guo, J., Yin, H. and Ning, P. (2015). Adsorption and oxidation of SO_2 by graphene oxides: A van der Waals density functional theory study. *Appl. Surf. Sci.* 324: 61–67.

Zhang, Y., Yuan, S., Feng, X., Li, H., Zhou, J. and Wang, B. (2016). Preparation of nanofibrous metal–organic framework filters for efficient air pollution control. *J. Am. Chem. Soc.* 138: 5785–5788.

Zhao, Q., Wu, F., Men, Y., Fang, X., Zhao, J., Xiao, P., Webley, P. and Grande, C. (2019). CO_2 capture using a novel hybrid monolith (H-ZSM5/activated carbon) as adsorbent by combined vacuum and electric swing adsorption (VESA). *Chem. Eng. J.* 358: 707–717.

Zhao, Y., Shen, Y., Ma, G. and Hao, R. (2014). Adsorption separation of carbon dioxide from flue gas by a molecularly imprinted adsorbent. *Environ. Sci. Technol.* 48: 1601–1608.

Zhao, Y., Liu, X. and Han, Y. (2015). Microporous carbonaceous adsorbents for CO_2 separation via selective adsorption. *RSC Adv.* 5: 30310–30330.

Zhao, Y., Wang, H. and Wang, T. (2016). Adsorption of NO from flue gas by molecularly imprinted adsorbents. *Chem. Eng. J.* 306: 832–839.

Zhao, Y., Wang, H. and Wang, T. (2017). Preparation of molecularly imprinted adsorbents and NO adsorption property. *Funct. Mater. Lett.* 10: 1650070.

Zhou, J., Wang, B., Nie, L., Lu, J., Hao, Y. and Xu, R. (2018a). Experimental study on emission of VOCs from tanker using hollow fiber membrane adsorption method with different absorbents. *IOP Conf. Ser.: Mater. Sci. Eng.* 292: 012113.

Zhou, L., Niu, Z., Jin, X., Tang, L. and Zhu, L. (2018b). Effect of lithium doping on the structures and CO_2 adsorption properties of metal-organic frameworks HKUST-1. *Chem. Select.* 3: 12865–12870.

Received for review, April 20, 2019
Revised, August 15, 2019
Accepted, August 16, 2019